GEOLOGICA CARPATHICA, 55, 1, BRATISLAVA, FEBRUARY 2004
19–36

STABLE ISOTOPE EVIDENCE FOR METER-SCALE SEA LEVEL CHANGES IN LOWER CRETACEOUS INNER PLATFORM AND PELAGIC CARBONATE SUCCESSIONS OF TURKEY

İSMAİL ÖMER YILMAZ[1], TORSTEN VENNEMANN[2], DEMİR ALTINER [1] and MUHARREM SATIR[2]

[1]Department of Geological Engineering, Middle East Technical University, 06531 Ankara, Turkey; ioyilmaz@metu.edu.tr
[2]Lehrstuhl für Geochemie, Institut für Mineralogie, Petrologie, und Geochemie, University of Tübingen, Wilhelmstraße 56, 72074 Tübingen, Germany

(Manuscript received November 26, 2002; accepted in revised form June 23, 2003)

Abstract: In this study, stable C and O isotope compositions of bulk rock samples from Barremian-Aptian platform carbonates of the Taurides, the Pontides, and of their pelagic counterparts of the Sakarya continent in Turkey were measured for the first time. Platform carbonates and pelagic successions including a prominent black shale interval are composed of distinct sedimentary cycles in the form of meter-scale shallowing- upward sequences and limestone-marl/shale couplets, respectively. The biostratigraphy and the $\delta^{13}C$ values allow this black shale interval to be correlated with the "Selli level". Variations in lithofacies and $\delta^{13}C$ and $\delta^{18}O$ values with the magnitudes of about 2 ‰ within the cycles indicate high frequency fluctuations in sea level, probably in response to alternate periods of cooling and warming occurring on Milankovitch-cycle scales even during the greenhouse-type Cretaceous. A good overall correlation between sedimentary cyclicity and variations in $\delta^{18}O$ values suggests preservation of the primary isotopic signal.

Key words: Barremian, Aptian, Taurides, Pontides, Sakarya, stable isotopes, cyclicity.

Introduction

Over the past decade, many studies have documented changes in sea level during the Early Cretaceous (e.g. Haq et al. 1988; De Boer & Smith 1994; Graciansky et al. 1998; Altıner et al. 1999; Raspini 2001; Pittet et al. 2002). Studies on the global climate indicate that greenhouse-type conditions existed during the Early Cretaceous, but that even within this type of climate, periods of prolonged cooling occurred (Weissert & Lini 1991; Sellwood et al. 1994; Pirrie et al. 1995; Barrera & Johnson 1999; Jenkyns & Wilson 1999; Price 1999; Stoll & Schrag 2000). While discussions on the ultimate cause of the climatic variation continue, correlations of both $\delta^{13}C$ and $\delta^{18}O$ values from different carbonate sequences of the Cretaceous justify a global interpretation and elucidate the controlling factors and scales of paleoclimatic and paleoceanographic changes (e.g. Menegatti & Weissert 1998; Larson & Erba 1999; Strasser et al. 2001).

The main purpose of this study is to document the relationship between stable isotope variations and meter- to larger-scale changes in sea level as documented by sedimentological, micropaleontological and petrographical features of both platform carbonates and pelagic successions of the eastern Tethyan margins. This study is part of a larger project dealing with sequence- and cyclostratigraphy of Barremian-Aptian sediments in the NW, WNW and SW of Turkey. First, an interpretation of the depositional environments of the observed facies and their cyclic patterns is presented; second, analysis of $\delta^{13}C$ and $\delta^{18}O$ data obtained from selected cycles and their interpretation in relation with sea level changes are given. This second part forms the core of this study. Detailed documentation of the high-resolution sequence-stratigraphic and cyclostratigraphic correlations of the sections are the topic of a continuing parallel study and will be published later.

Geological settings

This study covers three different regions: Taurus, Sakarya, and Zonguldak. Each region has its own specific geological setting.

A — The Taurus region in the southern part of Turkey is characterized by platform carbonates of the southern Neotethys Ocean. Of particular interest to this study is the Seydişehir area, where platform carbonates dominate (Figs. 1a, 1b, 2).

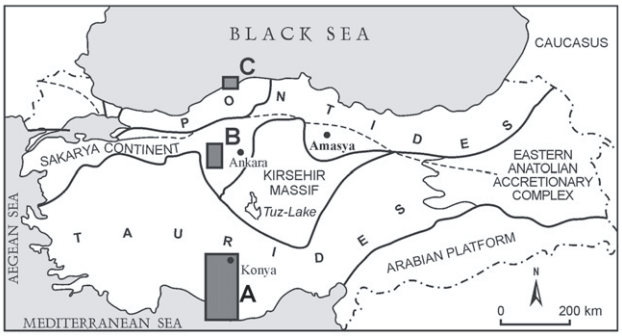

Fig. 1a. Geographic location of study regions (A, B, C). **A** — Taurus region (locality: Seydişehir area). **B** — Sakarya region (localities: Mudurnu and Nallıhan area). **C** — Zonguldak region (localities: Zonguldak, Kozlu and Çengellidere areas) (Yılmaz et al. 1997, modified).

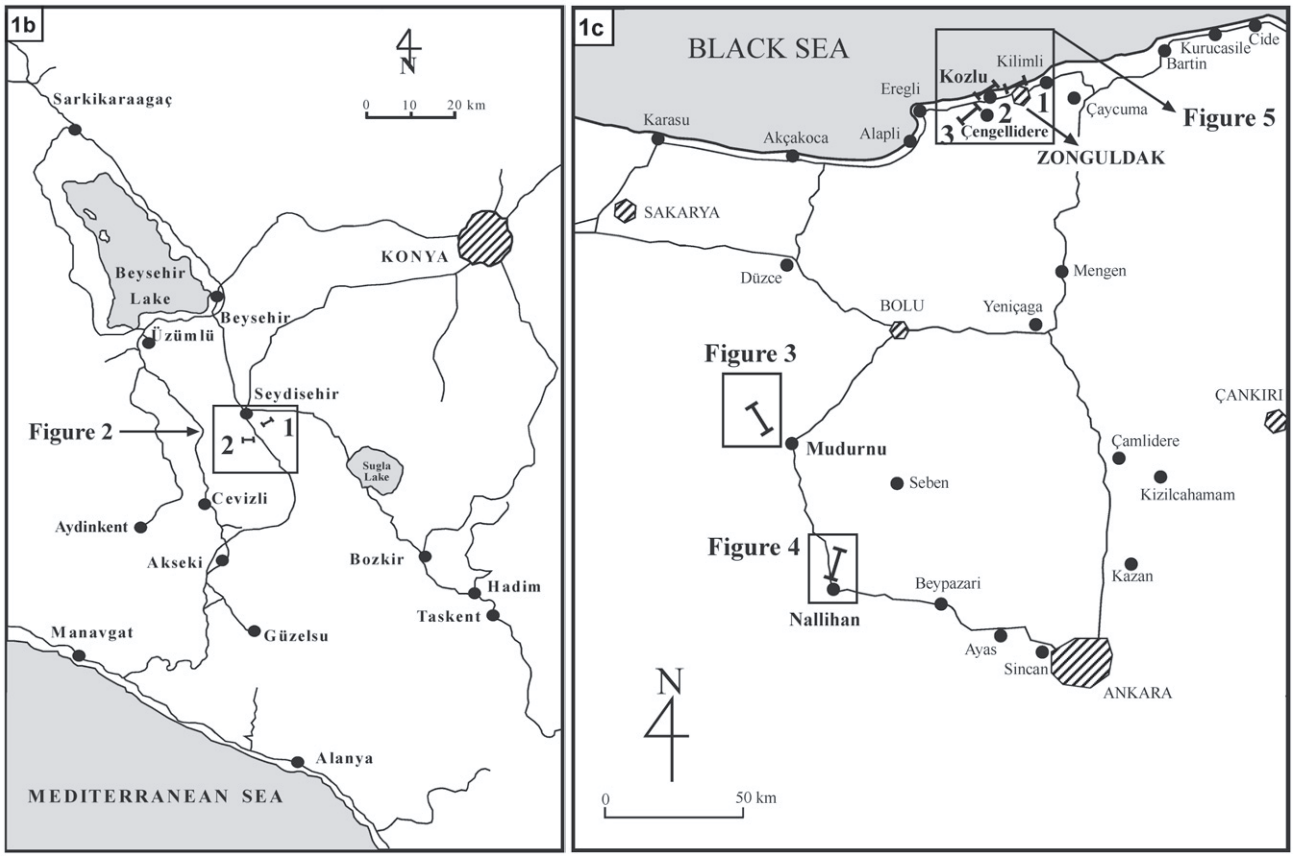

Fig. 1b–c. Geographic location of sections measured in the Seydişehir area in the Western Taurides (SW Turkey) (**b**). Geographic location of sections measured in the Mudurnu–Nallıhan (Sakarya) and Zonguldak (Pontides) areas (**c**).

The geology of this area has been studied extensively (Monod 1977; Özgül 1983, 1997; Altıner et al. 1999; Yılmaz 1999; Yılmaz & Altıner 2001). In the Seydişehir area (Fig. 2) typical autochthonous/para-autochthonous platform carbonates of the Taurides rest unconformably on sedimentary Cambrian-Ordovician and Triassic basement rocks. Shallow water platform carbonates ranging from Dogger to Paleocene in age form thick, relatively homogeneous successions over the basement rocks. Nappe movements during the Eocene resulted in prominent Eocene flysch successions covering much of the Taurides. Allochthonous units, which are generally composed of ophiolitic successions and underlying basement rocks, are unconformably covered by Neogene/Quarternary successions. Two stratigraphic sections have been studied, covering the Barremian–Aptian of the Polat Formation (Özgül 1997), which crops out extensively in the Western Taurides.

B — The Sakarya region is part of the so-called Sakarya continent (Şengör & Yılmaz 1981). Metamorphic basement and overlying Mesozoic and Cenozoic sedimentary and volcanic successions characterize the stratigraphy of the region. Paleozoic metamorphic basement rocks were overthrusted by Triassic sedimentary and metamorphic rocks during the Karakaya Orogeny. Liassic successions including "Ammonitico Rosso" facies unconformably overlie all these metamorphic suites and deformed sedimentary units. The rest of the Jurassic and Cretaceous successions start with alternations of shelf carbonates, pelagics, cherts, volcanics, and volcaniclastics, and continue with slope and basin deposits of the Upper Cretaceous. In the Mudurnu and Nallıhan areas studied, slope/basin pelagic carbonates dominate the successions (Figs. 1a, 3). These pelagics have been interpreted as deposits filling the intra-continental Mudurnu Trough of the Sakarya continent (Önal et al. 1988; Altıner et al. 1991; Altıner 1991; Altıner & Özkan 1991).

The two stratigraphic sections in the Nallıhan and Mudurnu areas include Lower Cretaceous pelagic carbonates of the Soğukçam Limestone (Figs. 1a, 1c, 3, 4). In the studied area, the Soğukçam Limestone is distinguished from other formations by the presence of limestone-shale/marl couplets.

C — The Zonguldak region is characterized by Cretaceous outcrops along the Western Black Sea Coast of Northwestern Turkey (Tokay 1954, 1955; Kaya et al. 1983; Derman 1990; Orhan 1995; Görür 1997). They represent a continental shelf facing towards an ocean in its south. In this region, Paleozoic rocks of the Western Pontides, composed of continental and shallow-water carbonates, are unconformably overlain by Jurassic-Cretaceous shallow-water carbonate-dominated successions, and followed by Upper Cretaceous flysch-type successions. The Zonguldak, Kozlu, and Çengellidere areas studied cover these Lower Cretaceous platform carbonates. Three stratigraphic sections have been investigated within the Öküsmedere and Çengellidere Formations (Figs. 1a, 1c, 5). The Öküsmedere Formation is composed of peritidal carbonates intercalated with thin siliciclastics. The Çengellidere Formation is the lateral extension of the Öküsmedere Formation, but also

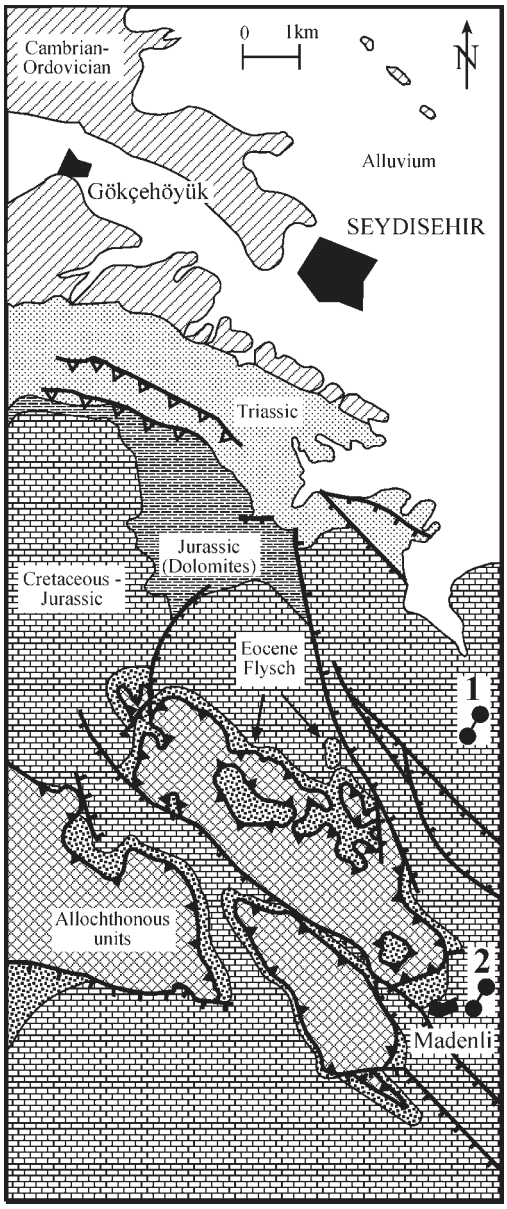

Fig. 2. Simplified and modified geological map of Seydişehir area (Monod 1977). The locations of measured sections are shown with numbers: **1** — Seydişehir-1; **2** — Seydişehir-Madenli.

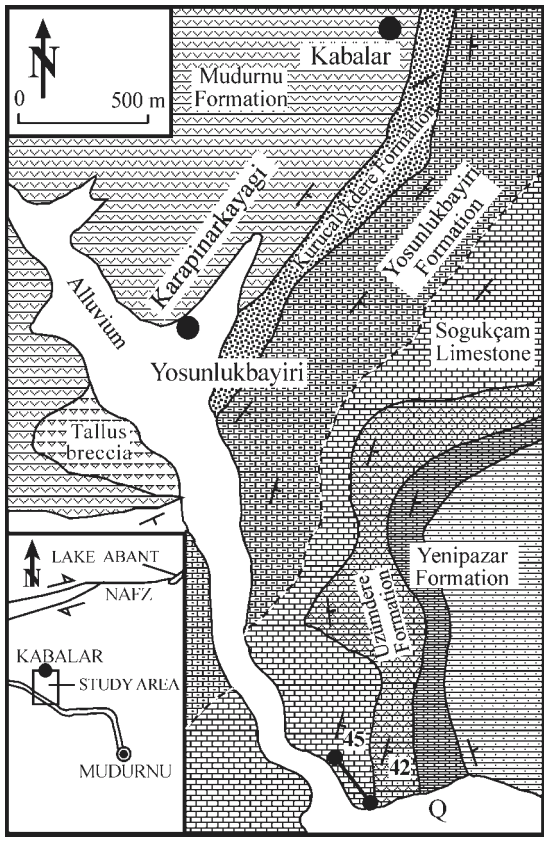

Fig. 3. Geological map of the Mudurnu (Sakarya) area (Altıner et al. 1991). The location of the measured section is shown with a bold line.

includes alternating reefal carbonates and thick siliciclastics. These two formations are separated from the Upper Jurassic to Lower Cretaceous Inaltı Formation by an unconformity, which is represented by red continental clastics of the İncigez Formation (Fig. 5).

Biostratigraphy and chronostratigraphy

Within the sections and on a regional basis the chronostratigraphy was established using benthic foraminiferal biozones in platform carbonates and planktonic foraminiferal biozones in pelagic successions (Altıner & Decrouez 1982; Derman 1990; Altıner 1991; Altıner et al. 1991, 1999; Altıner & Özkan 1991; Yılmaz 1999, 2002; Altıner & Yılmaz 2000; Yılmaz & Altıner 2001).

In the sections measured in the Zonguldak area (Pontides), two biozones (A and B) were established based on benthic foraminifers (Fig. 6). Zone A encompasses the interval between the uppermost Barremian and the Lower Aptian and is characterized by the total range of *Palorbitolina lenticularis.* Zone B is an assemblage zone corresponding to the Barremian and is characterized by *Orbitolinopsis debelmasi*, *Arenobulimina cochleata*, *Choffatella tingitana*, and *Orbitolinopsis flandrini.* In the sections measured in the Mudurnu and Nallıhan areas (Sakarya), the Barremian-Aptian boundary is defined between the *Hedbergella sigali* and *Hedbergella similis* Interval Zones. The Aptian is divided into 7 zones by the successive appearances of *Hedbergella similis*, *Globigerinelloides blowi, Leopoldina cabri, Globigerinelloides ferroelensis, Globigerinelloides algerianus* and *Planomalina cheriiourensis* (Fig. 6). In the Nallıhan section, the *Planomalina cheriiourensis* Zone is not recorded due to truncated uppermost part of the section by a thrust fault in the area. In the sections measured in the Seydişehir area (Taurides), the studied successions correspond to the K2b and K3 Zones of Altıner et al. (1999). Zone K2 is characterized by the *Vercorsella scarsellai–Salpingoporella dinarica* Assemblage Zone and covers the Upper Hauterivian–Lower Aptian interval. K2b is the *Voloshinoides murgensis* Subzone defined within the K2 Zone and corresponds to the Lower Aptian (Fig. 6). Zone K3 is characterized by *Cuneolina* gr. *pavonia* — Miliolidae 1 assemblage and encompasses the interval between the Upper Aptian to Cenomanian. All the biozones are correlated with

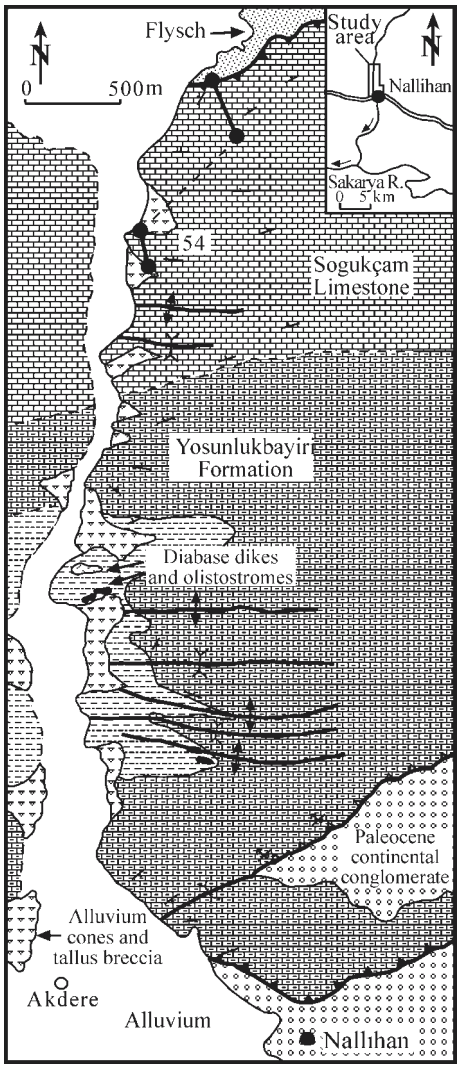

Fig. 4. Geological map of the Nallıhan (Sakarya) area (Altıner et al. 1991). The locations of measured sections are shown with numbers.

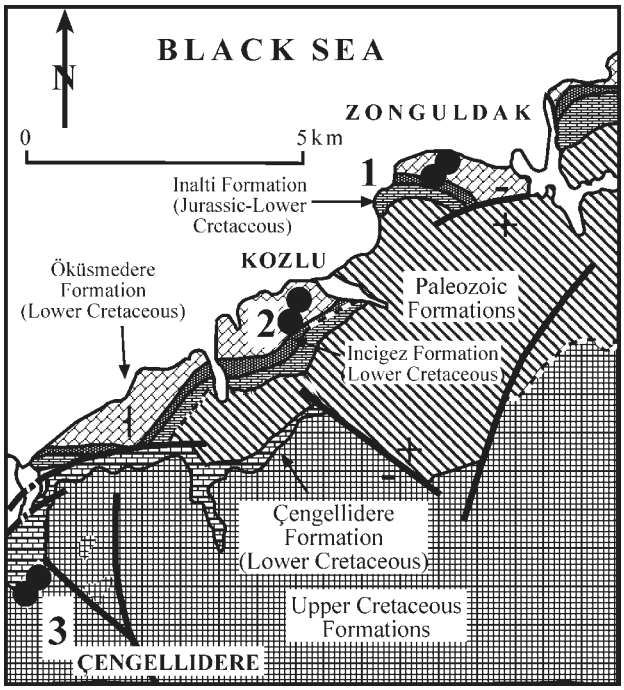

Fig. 5. Generalized geological map of the Zonguldak and surrounding areas (simplified from Derman 1990). Locations of the measured sections are shown with numbers: **1** — Zonguldak; **2** — Kozlu; **3** — Çengellidere.

the biozones in the biostratigraphic chart of Graciansky et al. (1998). The approximate durations of zones will be used for a rough calculation of the duration per cycle in the studied sections. The upper and lower boundaries of the studied sections do not coincide with stage boundaries because of limited exposure. Therefore, the dates attributed to the base and the top of the sections are approximated.

Cyclic stratigraphy of the sections methodology

A total of five outcrop sections were measured in the Seydişehir (Taurides), Sakarya (Sakarya), and Zonguldak (Pontides) regions of Turkey. All the studied sections have been measured bed-by-bed in the field and sampled at a meter or sub-meter-scale. Semi-quantitative analysis of 448 thin sections and hand samples was performed in the laboratory to define microfacies types. Bedding surfaces, sedimentary structures, weathering profiles, and facies compositions were identified in the field. Vertical and lateral facies changes, associations of micro- and macro-sedimentary structures, and microfacies types are used in the reconstruction of cyclicity. Sedimentary cyclicity is recorded as shallowing-upward meter-scale cycles in inner platform settings, and as limestone-marl/shale couplets in pelagic settings. The Seydişehir and Zonguldak sections represent inner platform carbonates, whereas pelagic successions are represented by the Nallıhan and Mudurnu sections.

Inner platform carbonates

Taurides — Seydişehir sections

In the Seydişehir area, two stratigraphic sections, Seydişehir-1 and Seydişehir-Madenli have been studied in detail. They are separated by a distance of 2 km (Figs. 1b, 2). The Seydişehir-1 section has a thickness of 36.03 m and covers the Early Aptian–Late Aptian/Albian time interval (Fig. 7). The Seydişehir-Madenli section covers the Aptian period and is 15.37 m thick (Fig. 8). The sections are composed of a continuous succession of shallowing-upward meter-scale cycles (Altıner et al. 1999; Yılmaz & Altıner 2001) (Figs. 7, 8). Cyclicity is mainly defined by the vertical arrangement of subtidal, intertidal, and supratidal facies. Cycles generally start with intraclastic, peloidal, foraminiferal, dasyclad algal pack- to wackestones of a shallow subtidal environment and continue vertically with algal, foraminiferal lime mud- to wackestone facies. They are capped by cryptalgal laminites/stromatolites, or fenestral limestones of intertidal/supratidal environments. The top of each cycle is generally characterized

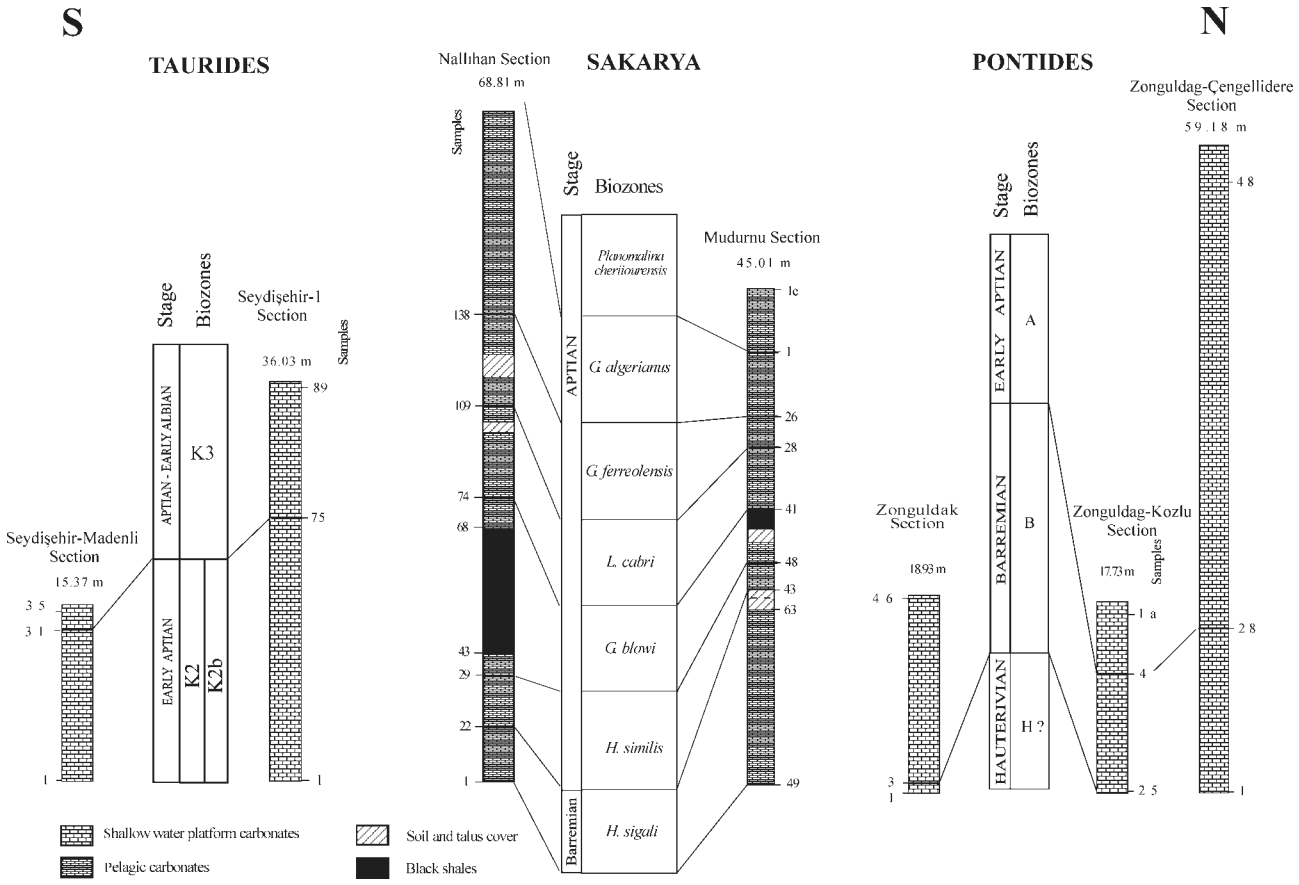

Fig. 6. Biostratigraphic framework including biozones determined in the Zonguldak, Mudurnu and Nallıhan, and Seydişehir sections and their correlation. (Biozones are exactly equal to biozones determined in Altıner et al. (1999), Yılmaz (1999, 2002).)

by subaerial exposure features such as karstic breccias and dissolution vugs (Demicco & Hardie 1994; Altıner & Yılmaz 2000; Yılmaz et al. 2000; Yılmaz & Altıner 2001). Therefore, each cycle is represented by an asymmetrical transgressive-regressive sequence (Strasser 1991). Transgressive and regressive portions of the cycles reflect transgressive and highstand conditions of small scale sea level changes. Records of lowstand condition may be reworked in transgressive phase or hidden in the subaerial exposure structures. A predominantly shallowing-upward nature is consistently recorded in both sections. The shallowing-upward cycles resemble the "small-scale sequences" of Strasser et al. (1999). The thicknesses of cycles range between 1 m and 1.5 m. The durations can be calculated simply by dividing the time interval represented in the section by the number of cycles detected, assuming that each cycle has the same duration and that there are no gaps. The estimated approximate durations of the parts of the stages covered in the sections are about 1–2 Ma for the Seydişehir-Madenli section and 2–4 Ma for the Seydişehir-1 section, according to the correlation of the biostratigraphic framework in the sections with the chronostratigraphic charts of Haq et al. (1988) and Graciansky et al. (1998). Thus, the duration per cycle in the Seydişehir-1 section ranges between 74 Ka and 148 Ka, and between 62.5 Ka and 125 Ka in the Seydişehir-Madenli section (Table 1). These durations are close to the 100 Ka of the first eccentricity cycle (Fischer 1991), suggesting that sea level changes were related to changes in the Earth's orbital parameters. Similar patterns of cyclicity and durations of cycles are described by Pittet et al. (2002) from Barremian-Aptian successions of northern Oman.

Table 1: Table showing the calculated durations per cycles in measured sections and comparison with the frequencies in Milankovitch band.

Name of the section	Time interval of the section	Number of cycles	Calculated duration per cycle	Milankovitch cyclicity
Seydişehir-1	2–4 Ma	27	Between 74–148 Ka	Eccentricity signals (E1 and E2)
Seydişehir-Madenli	1–2 Ma	16	Between 62.5–125 Ka	Obliquity and eccentricity signals (E1 and E2)
Zonguldak	3–4 Ma	43	Between 70–93 Ka	Eccentricity signal (E1)
Zonguldak-Kozlu	1–2 Ma	8	Between 125–250 Ka	Eccentricity signal of E2
Zonguldak-Çengellidere	1–2 Ma	21	Between 48–95 Ka	Obliquity and eccentricity signal of E1
Mudurnu	6–7 Ma	122	Between 49–57 Ka	Obliquity signal
Nallıhan	4–5 Ma	117	Between 34–43 Ka	Obliquity signal

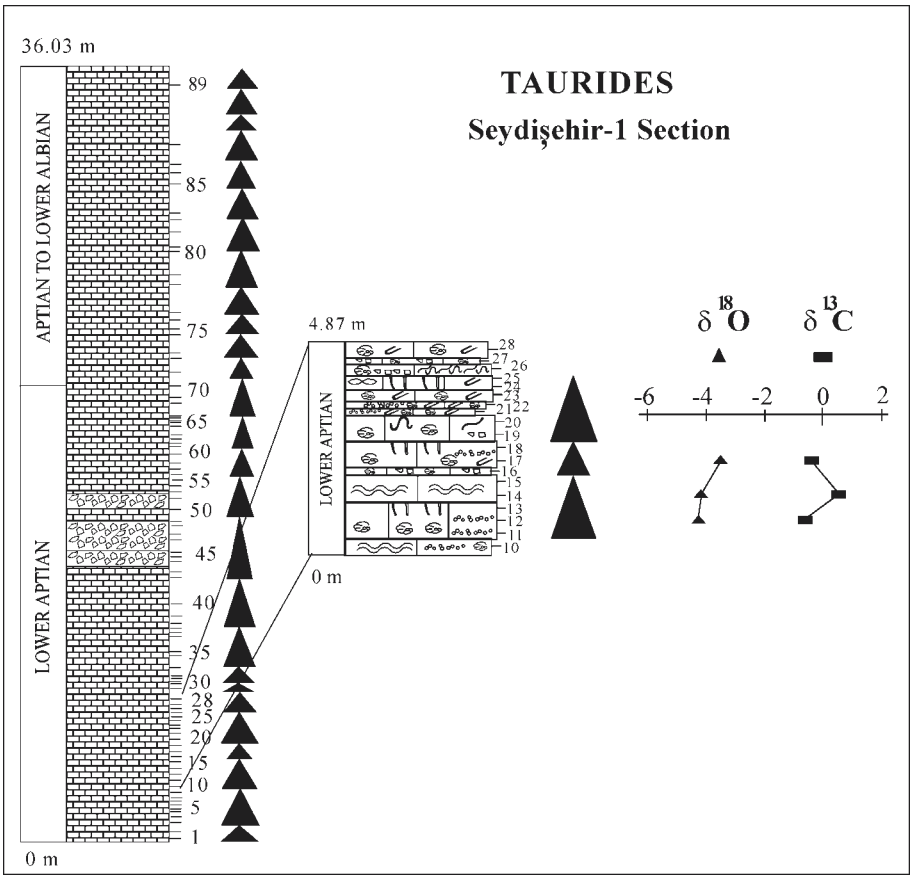

Fig. 7. Shallowing-upward meter-scale cycles and stable isotope variations within the cycles of the Seydişehir-1 section (for symbols see Legend to Fig. 7).

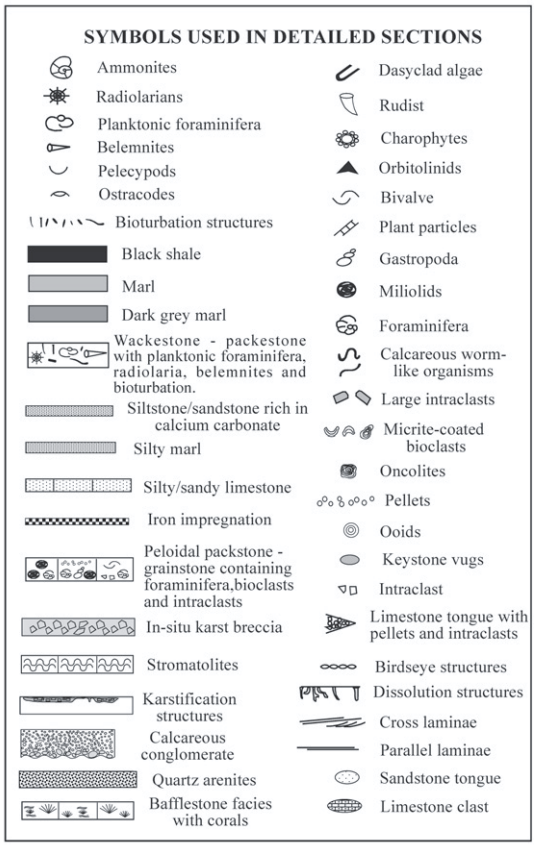

Legend to Fig. 7.

Pontides — Zonguldak sections

The Zonguldak sections studied (Zonguldak, Zonguldak-Kozlu, Zonguldak-Çengellidere) are well-exposed outcrops of inner platform carbonates and their siliciclastic intercalations. The Zonguldak and Zonguldak-Kozlu sections represent parts of the Öküsmedere Formation, whereas the Zonguldak-Çengellidere section is part of the Çengellidere Formation (Fig. 5) (Derman 1990; Orhan 1995; Görür 1997). Distances between the sections are about 3 to 5 km (Fig. 5).

The Zonguldak and Zonguldak-Kozlu sections have very similar features and complement each other. The Zonguldak section has a thickness of 18.93 m and covers the Late Hauterivian–Barremian period. The Zonguldak-Kozlu section is 17.73 m thick and covers the Late Barremian–Aptian time interval (Figs. 9, 10).

In both sections, cyclicity is defined by vertical facies arrangements. Cyclicity is recorded as an alternation of thinner limey sandstones or sandy limestones/siltstones and thicker limestones. Sandstones and siltstones occur at the bottom of each cycle and are interpreted to represent lowstand and/or transgressive conditions. They are overlain by limestones deposited during highstand condition of cycles (Osleger 1991; Strasser 1999). Sandstones and siltstones are generally composed of quartz, benthic foraminifers, dasyclad algae, plant particles, and carbonate matrix. Within the siliciclastics, faint laminations are also observed. Limestones constitute bioclastic, peloidal, foraminiferal, dasyclad algal pack- and wacke-

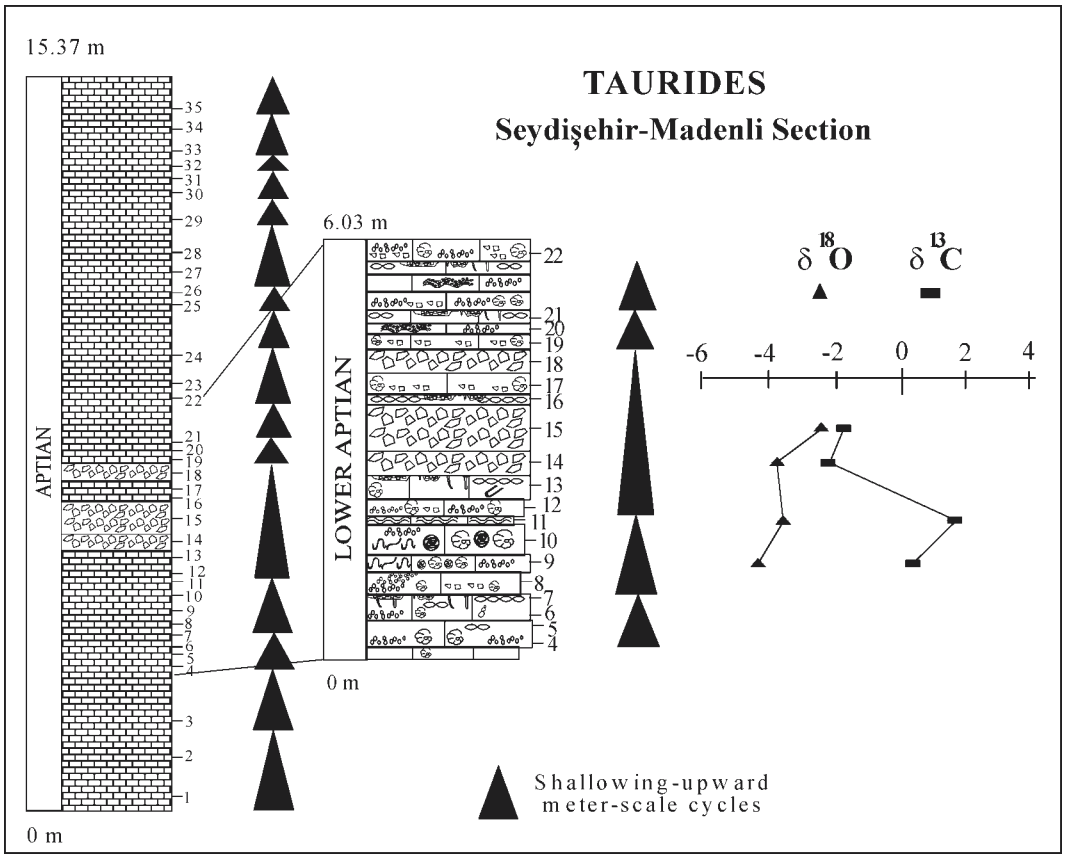

Fig. 8. Shallowing-upward meter-scale cycles and stable isotope variations within the cycles of the Seydişehir-Madenli section (for symbols see Legend to Fig. 7).

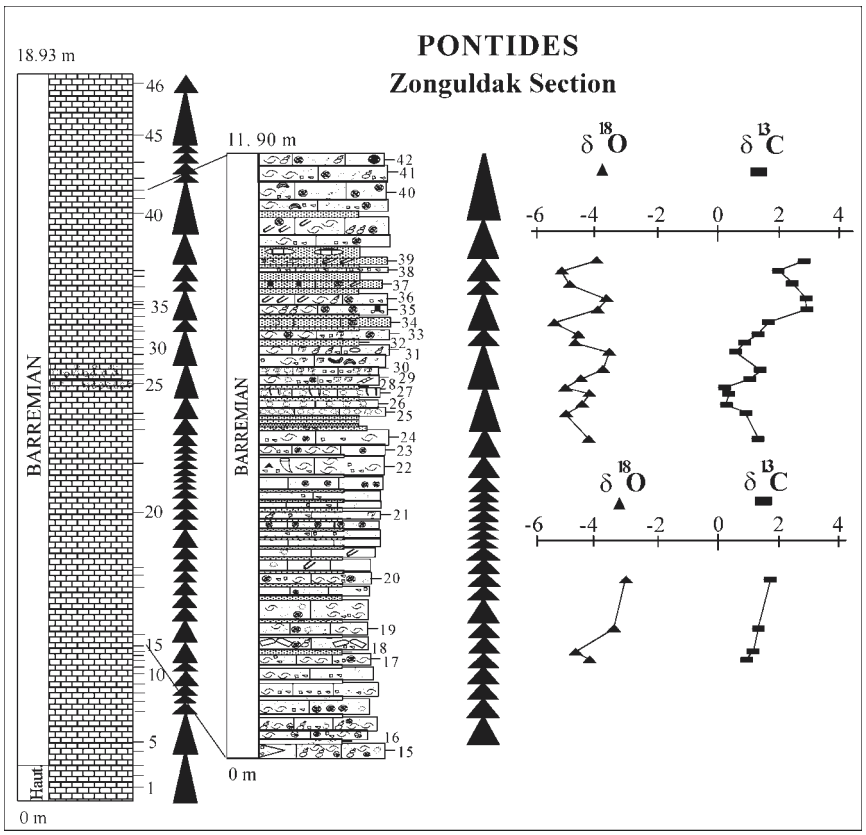

Fig. 9. Shallowing-upward meter-scale cycles (sandstone-limestone couplets) and stable isotope variations within the cycles of the Zonguldak section (for symbols see Legend to Fig. 7).

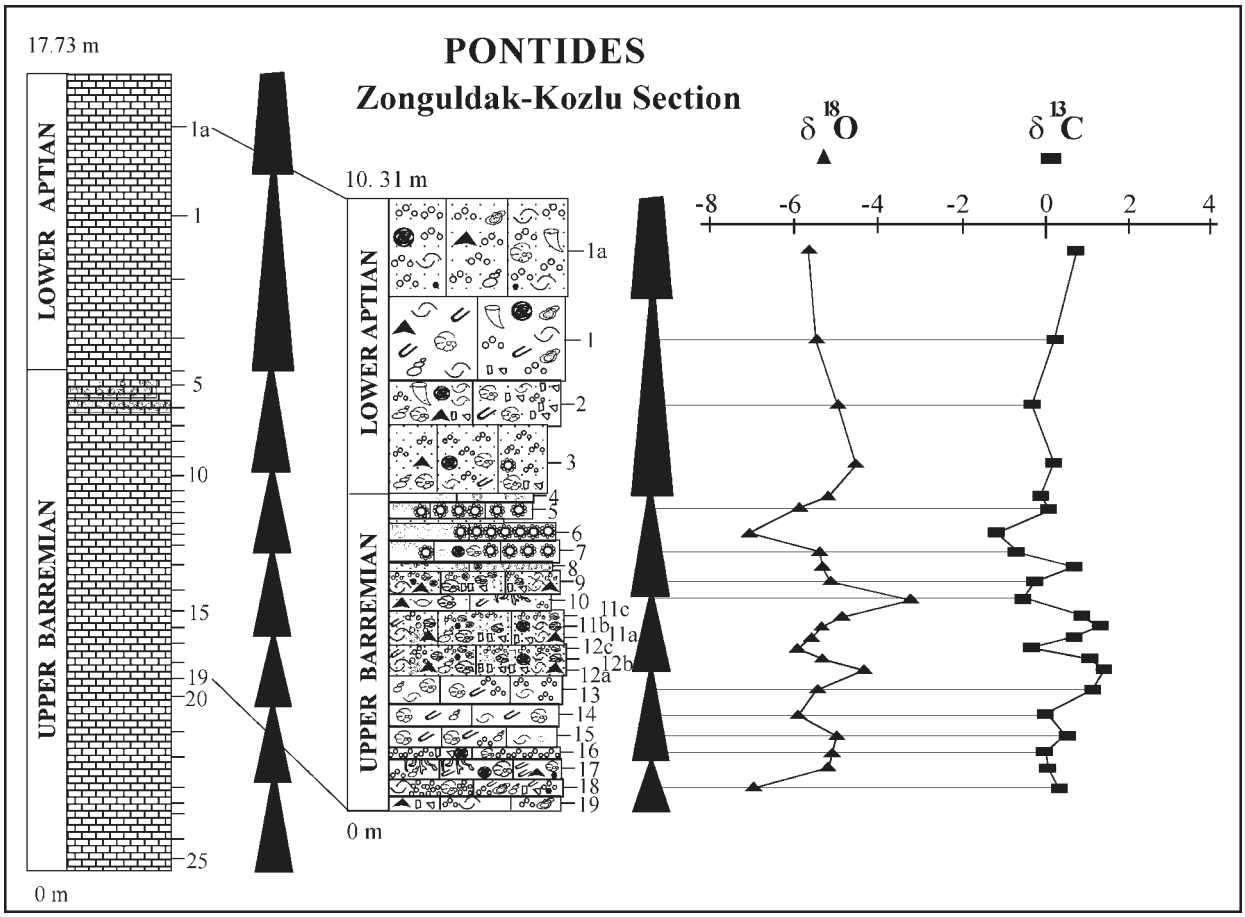

Fig. 10. Shallowing-upward meter-scale cycles (sandstone-limestone couplets) and stable isotope variations within the cycles of the Zonguldak-Kozlu section (for symbols see Legend to Fig. 7).

stones. Lime mudstones and charophyte packstones are infrequently intercalated (Fig. 9).

In both sections, cycles do not exhibit subaerial exposure structures but instead are more like "submerged cycles" (Altıner et al. 1999) or "subtidal cycles" of Osleger (1991). In a few cycles, dissolution vugs filled with vadose silts are recorded and overlain by sandy beds including clasts derived from the lower units. Some caliche clasts are also recorded in these sandstones. Consequently, the bases of the sandstones are interpreted as ravinment surfaces. In addition, the limestones contain fragments of rudists and other bivalves increasing in proportion relative to the sandstones.

In contrast to the Zonguldak section, the Zonguldak-Kozlu section represents a less sandy succession. The cycles start with sandy limestones and/or peloidal wackestones/packstones and end with thicker pure limestones having bioclastic, peloidal, foraminiferal, dasyclad algal packstones/wackestones or grainstones at the top. In both sections, a prominent charophyte packstone level composed of successive beds is recorded. This level is interpreted as a record of a sea level still-stand and/or fall in the sea level. The charophyte packstone occurs at the top of the cycles and overlies siltstones/sandstones at the bottom of the cycles. This also supports the view that limestone-sandstone couplets are formed by shallowing-upward conditions (Fig. 10).

The Zonguldak–Çengellidere section covers the Early Aptian period and has a thickness of 59.18 m (Fig. 11). This section has more siliciclastic intercalations within its succession, compared to the Zonguldak and Zonguldak-Kozlu sections. Thick cross-bedded calcareous sandstones, quartzarenites, calcareous conglomerates, and pebbly sandstones occur in the lower to middle parts of the section. Some black mudstones and siltstones alternating with sandstones are also observed. This section is composed of shallowing-upward meter-scale cycles. In this section two types of cycles are observed: conglomerate-sandstone couplets and sandstones/sandy limestone–limestone couplets. Conglomerates occur at the bottom and sandstones at the top of these siliciclastic cycles, representing fining-upward cycles. Sandstones and sandy limestones form the bottom part and limestones composed of bioclastic packstone, peloidal, foraminiferal wackestone/packstone or even bafflestone facies form the upper part of the sandstone-limestone cycles (Fig. 11). In all cycles, subaerial exposure structures are not recorded. In all conglomerates and sandstones, except in the quartzarenites alternating with conglomerates and sandstones, in situ benthic foraminifers are found. Therefore, the cycles in Zonguldak sections are interpreted as "submerged cycles" (Altıner et al. 1999) in this study. Because of the thick sandstones and conglomerates, average cycle thickness rises up to 3 m in this section.

As in the Tauride sections, the duration of each cycle is calculated by dividing the time interval represented in the section by the number of cycles detected. (The estimated rough approximate durations of part of the stages covered in the sec-

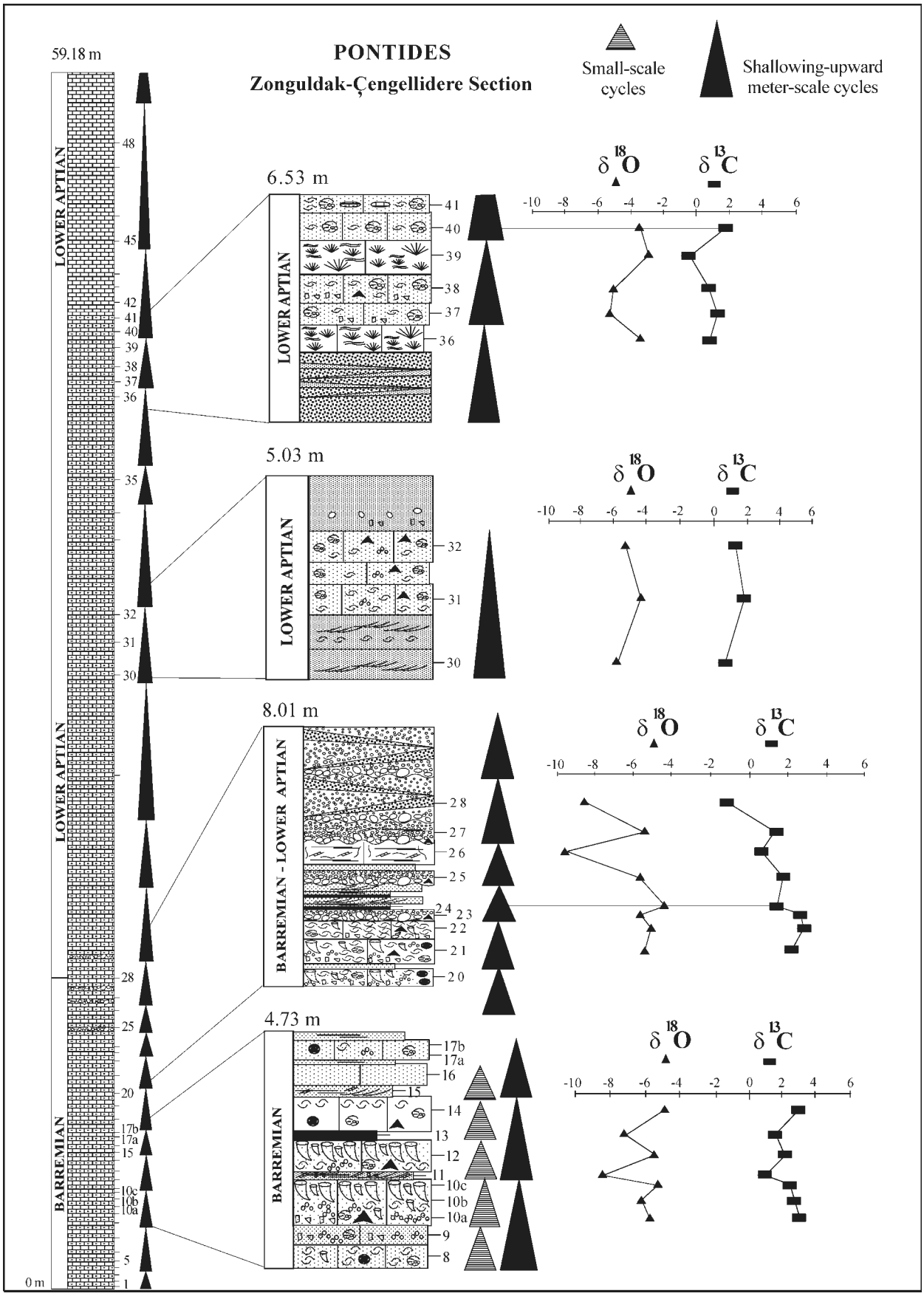

Fig. 11. Shallowing-upward meter-scale cycles (sandstone-limestone couplets) and stable isotope variations within the cycles of the Zonguldak-Çengellidere section (for symbols see Legend to Fig. 7).

tions are about 3–4 Ma for Zonguldak section, and 1–2 Ma for Zonguldak-Kozlu section, and 1–2 Ma for Zonguldak-Çengellidere section after the correlation of the biostratigraphic framework in the sections with the global sea level chart (Haq et al. 1988 and Graciansky et al. 1998).) The duration of each cycle on the sections fits to the orbital eccentricity of the Milankovitch band, E1 (98 Ka) and E2 (126 Ka) signals of Fischer (1991) (Table 1) indicating that sea level changes were related to changes in Earth's orbital parameters.

Additionally, smaller-scale cycles have been observed within meter-scale cycles. These cycles are fining-upward within a particular bed or form repetitions of thin sandy/clayey beds with limestone beds (Fig. 11). Although grouping and ordering of the smaller scale cycles are still in progress, it is found that 2 or 3 of them form a bundle within one meter-scale cycle in the Zonguldak-Çengellidere section (Fig. 11 — lower detailed section). However, the distribution of these cycles is rather random compared to the meter-scale cycles. Further studies are required to interpret these cycles.

Pelagic carbonates

Sakarya — Nallıhan and Mudurnu sections

Both sections comprise the pelagic counterparts of the studied Barremian-Aptian shallow water carbonates of Seydişehir and Zonguldak regions. The Nallıhan section has a thickness of 68.81 m, whereas the Mudurnu section is 45.01 m thick (Figs. 12, 13). The distance between the two sections is about 50 km. Both sections occur within pelagic carbonates overlying successions of the Mudurnu Trough with a large transgression (Altıner 1991; Altıner & Özkan 1991; Altıner et al. 1991). They are composed of cm to m scale cycles represented by limestone-marl/shale couplets. The regular alternation of couplets throughout the sections is impressive on the outcrop scale and indicates a relatively homogeneous cyclicity.

Limestones composed of planktonic foraminiferal, radiolarian wackestone/packstone facies form the top of the cycles, whereas marls and shales with some radiolarians and planktonic foraminifers form the bottom of the cycles. A prominent black shale interval is recorded in both sections. It occurs within the *G. blowi* Zone, and is interpreted as equivalent of the "Selli level" (Wezel 1985) (Figs. 12, 13). It is 11 m thick in the Nallıhan section and 2 m in the Mudurnu section. These differences in thickness might be related to paleotopographic conditions. In the Nallıhan section, the black shales are well exposed. The black shale interval displays cm- to m-scale cycles, which are generally composed of marl-shale couplets (Yılmaz et al. 2000) (Figs. 12, 13). Within the black shale, presence of thin glauconitic sandstone beds rich in quartz and feldspars, relatively ammonite-rich marls and iron enrichment suggest that this interval is a condensed section deposited during a maximum transgression of sea level (Yılmaz et al. 2000; Yılmaz 2002). Similar records are also described in Martire (1992), Peybernes et al. (2000), Prokoph & Thurow (2001), Vennin & Aurell (2001), Hesselbo & Huggett (2001) and in many others. Boundaries between limestones and marls/shales are transitional. Bioturbations in the limestones are followed by shales and marls. Decreasing clay contents in limestones,

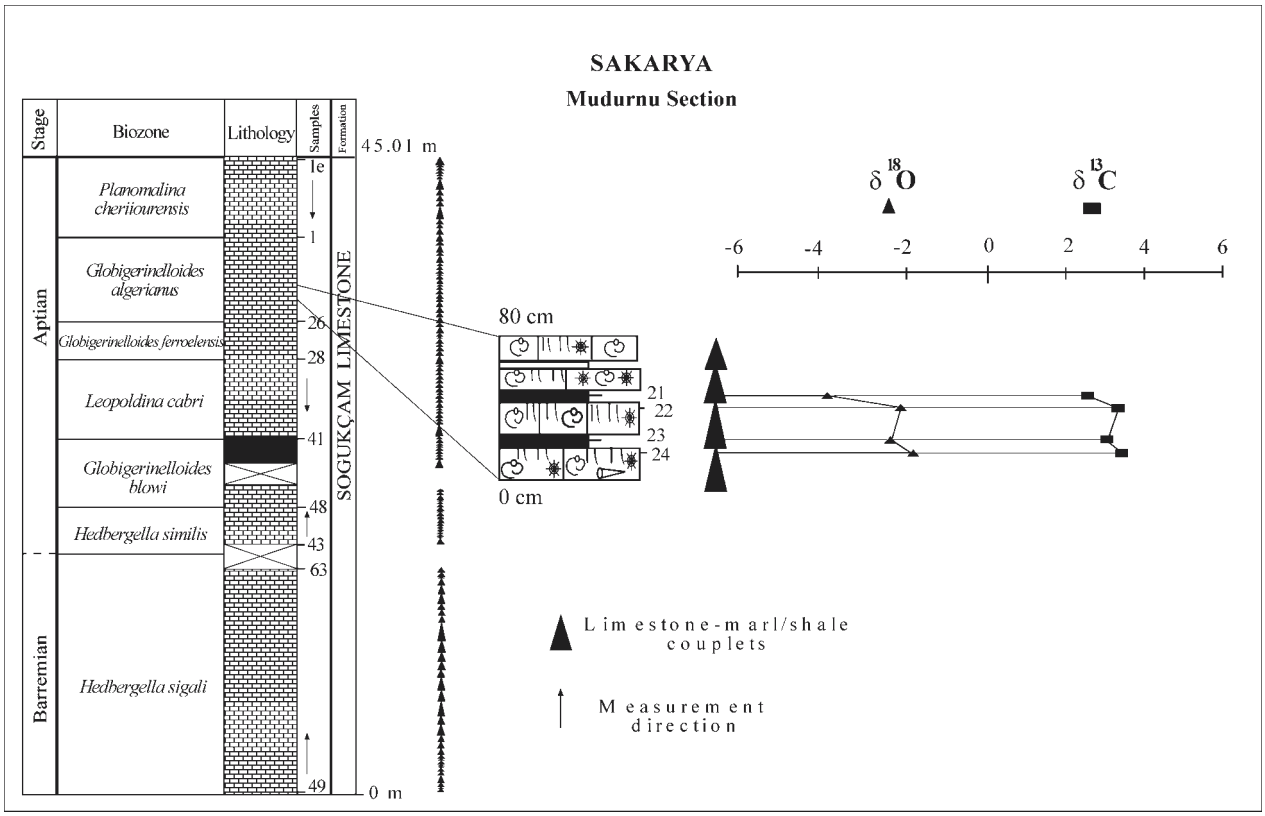

Fig. 12. Limestone-marl/shale cycles, black shale interval and stable isotope variations within the cycles of the Mudurnu section (for symbols see Legend to Fig. 7).

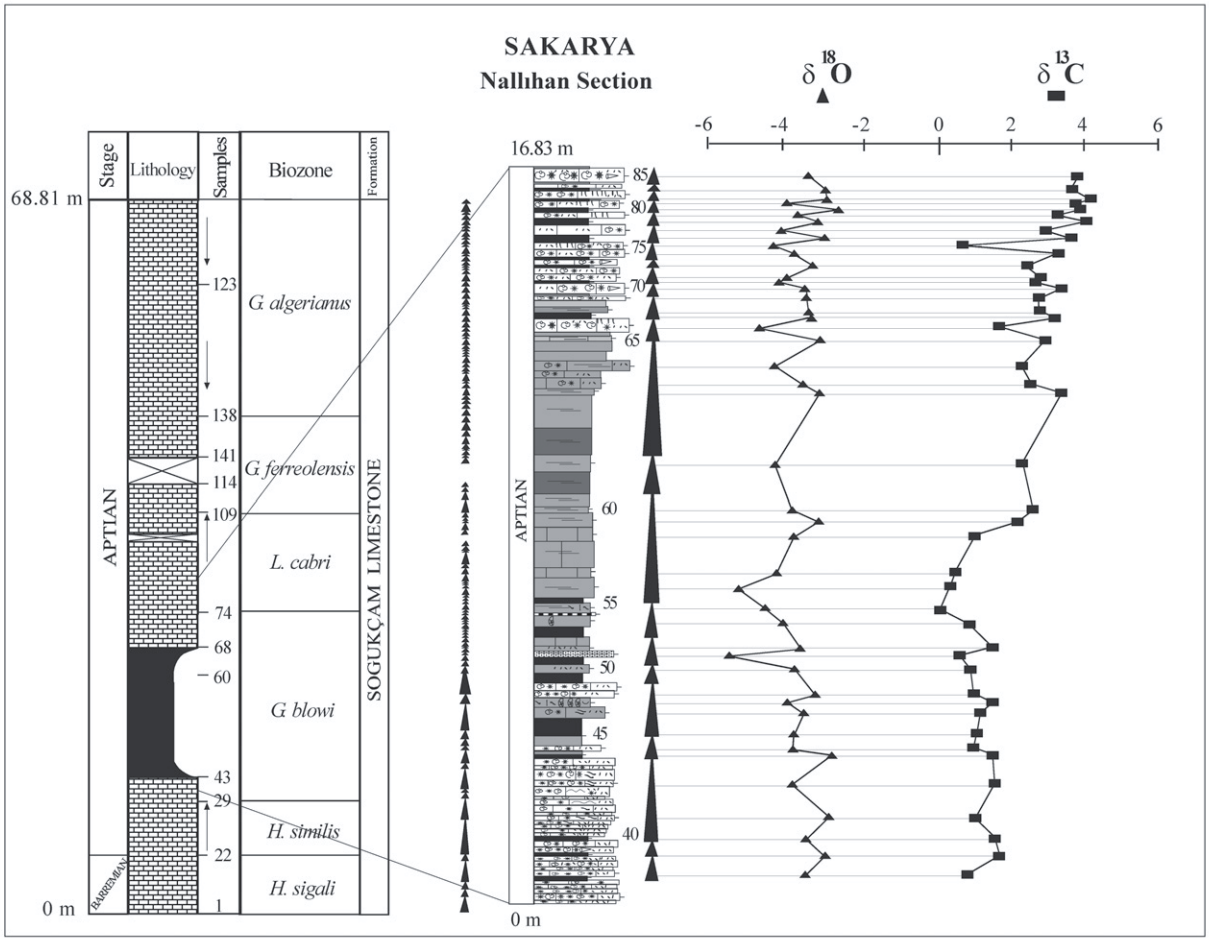

Fig. 13. Limestone-marl/shale cycles, black shale interval and stable isotope variations within the cycles of the Nallıhan section (for symbols see Legend to Fig. 7).

and comparison of the position of the black shale within limestone-marl/shale couplets with black shale intervals overlain by the pelagic limestones in both sections, which are already interpreted as a transgressive record in the large-scale, lead to the interpretation that the thin marls and black shales were deposited due to small-scale transgressions (Yılmaz et al. 2000 and Yılmaz 2002). The thin transggressive shales and marls are also described by Bralower et al. (1994, 1999), Claps & Masetti (1994), Claps et al. (1995), Bellonca et al. (1996). Similarly, Mutterlose & Ruffell (1999) indicated the position of dark marls deposited in transgressive and pale marls deposited in high stand conditions of sea level within the Hauterivian-Barremian deposits of Eastern England and Northern Germany. The limestone beds are commonly bioturbated and filled with black, grey clayey material derived from overlying black shales/marls. Therefore, limestones are set at the tops of cycles and interpreted as records of sea level high stand. The limestone-marl/shale couplets are interpreted as the records of small-scale sea level changes induced by climatic effects (as in Claps & Masetti 1994; Claps et al. 1995; Yılmaz et al. 2000; Pittet et al. 2002; Yılmaz 2002 and many others).

As in the Seydişehir and Zonguldak sections, the duration of each cycle is similarly calculated by dividing the time interval of the whole section by the number of cycles detected. (The approximate durations of part of the stages covered in the sections are about 1–2 Ma for Barremian and 5 Ma for Aptian in Mudurnu section and 4–5 Ma for Aptian in the Nallıhan section after the correlation of biostratigraphic framework in the sections with the global sea level chart (based on time-scales of Haq et al. 1988).) The duration of each cycle in the sections fits the axial obliquity of the Milankovitch band, with a model period of 41 Ka of Fischer (1991) (Table 1) indicating that sea level changes were related to changes in the Earth's orbital parameters.

However, on the basis of the time-scale of Graciansky et al. (1998) and Premoli Silva & Sliter (1999), the approximate duration for the Aptian represented in the Mudurnu section is about 8–8.8 Ma, and 7–8 Ma in the Nallıhan section.

Therefore, the duration per cycle in pelagic sections gives a range between 45 Ka and 76 Ka, depending on the different time-scales used.

Stable isotope analysis

Methodology

Because of the lithified texture, and fine-grain size of the samples, all stable isotope analyses were obtained from bulk rock samples. Individual foraminiferal species or other micro-

fossils could not be separated. During the sampling, the fine-grained matrix and homogeneous micritic parts of limestones were used and, unless specifically sampled for, care was taken to avoid larger clasts and veins. Powders were obtained from well-polished surfaces of hand specimens by means of a hand-held drill. Two milligrams of powdered sample collected from several spots of the sample slab were homogenized, washed with 2.5% NaOCl for 24 hours and rinsed several times with distilled water. Samples were subsequently dried at 70 °C overnight.

Isotopic compositions were measured at the University of Tübingen using an automated GasBench II online to a Finnigan MAT 252 mass spectrometer, and He carrier gas. Samples of about 100 µg size were dissolved by several drops of orthophosphoric acid (100%) at 70 °C in individual borosilicate glass vials. Isotopic compositions are expressed as conventional δ-values in permil (‰) relative to V-PDB. Precision is about 0.08 ‰ and accuracy 0.1 ‰ for both oxygen and carbon. The isotopic ratios were normalized relative to the in-house standard (Laaser Marble, with $\delta^{13}C$ = +1.5 ‰ and $\delta^{18}O$ = –5.2 ‰, calibrated against NBS-19 $\delta^{13}C$ = +1.95 ‰, and $\delta^{18}O$ = –2.20 ‰). A total of 126 bulk rock samples, 15 vein samples, 5 shell samples, 8 samples from visibly bioturbated parts, 4 infilling samples, and 6 clast samples have been analysed.

Table 2: Carbon and oxygen stable isotope values of bulk carbonate rock samples, veins, infillings, bioturbations, shells and corals obtained from measured sections in this study.

Nallıhan Section					
Samp. N.	$\delta^{13}C$	$\delta^{18}O$	Type	$\delta^{13}C$	$\delta^{18}O$
YN-38	0.95	-3.52			
YN-39	1.81	-3.01	Biot.	1.37	-3.76
YN-40	1.76	-3.46			
YN-41	1.14	-2.94			
YN-42	1.75	-3.65			
YN-43	1.65	-2.93	Biot.	2.02	-2.76
YN-44	0.98	-3.89			
YN-45	0.83	-3.87	Biot.	1.36	-3.72
YN-46	1.13	-3.80	Biot.	1.37	-3.71
YN-47	1.47	-3.93	Vein	-0.10	-5.89
YN-48	1.23	-3.25	Vein	1.20	-6.46
YN-50	0.95	-3.93			
YN-51	0.86	-5.32			
YN-52	1.35	-3.78			
YN-53	0.78	-4.05			
YN-55	0.01	-4.41			
YN-56	0.08	-5.03			
YN-57	0.39	-4.05			
YN-58	0.82	-3.84			
YN-59	2.16	-3.27			
YN-60	2.48	-3.86			
YN-61	2.34	-4.05			
YN-62	3.31	-3.31			
YN-63	2.44	-3.70			
YN-64	2.25	-4.04			
YN-65	2.90	-3.34	Biot.	3.72	-3.54
YN-66	1.93	-4.68			
YN-67	3.27	-3.18			
YN-68	2.69	-3.71			
YN-69	2.55	-3.74	Biot.	2.43	-3.66
YN-70	3.38	-3.47			
YN-71	2.53	-4.01			
YN-72	2.59	-3.76	Biot.	1.24	-4.50
YN-73	2.44	-3.23			
YN-74	3.31	-3.70			
YN-75	0.59	-4.12			
YN-76	3.56	-2.87			
YN-77	2.99	-4.00			
YN-78	4.01	-3.10			
YN-79	3.25	-3.58	Biot.	2.80	-4.08
YN-80	3.87	-2.60			
YN-81	3.68	-3.85			
YN-82	4.18	-2.85			
YN-84	3.63	-2.86			
YN-85	3.78	-3.43			
Average	2.11	-3.64			

Seydişehir-1 Section					
Samp. N.	$\delta^{13}C$	$\delta^{18}O$	Type	$\delta^{13}C$	$\delta^{18}O$
OS-12	-0.81	-4.39	Vein	-4.13	-7.23
OS-14	0.28	-4.06	Vein	-1.35	-4.23
OS-17	-0.16	-3.82			
OS 74	-2.09	-4.06	Vein	-5.18	-5.15
			Clast	-0.47	-3.60
Average	-0.23	-4.09			
Seydişehir-Madenli Section					
Samp. N.	$\delta^{13}C$	$\delta^{18}O$	Type	$\delta^{13}C$	$\delta^{18}O$
OSM 9	0.30	-4.23			
OSM-11	1.71	-3.67	Vein	-3.23	-6.35
OSM 14	-2.26	-3.73	Vein	-4.54	-6.74
			Clast	-1.50	-3.46
OSM-15	-1.84	-2.57	Clast	-3.07	-3.40
OSM-31a	-1.05	-3.78	Clast	-1.07	-3.97
OSM 31b	-0.74	-3.25	Clast	-0.89	-3.69
Average	-0.52	-3.55			
Zonguldak Section					
Samp. N.	$\delta^{13}C$	$\delta^{18}O$	Type	$\delta^{13}C$	$\delta^{18}O$
OZ-17	1.01	-4.16			
OZ-18	1.10	-4,47	Clast	0.04	-5.10
OZ-19	1.34	-3.44			
OZ-20	1.82	-3.31			
OZ-24	1.16	-4.05			
OZ-25	0.85	-5.00	Vein	-0.47	-7.24
OZ-26	0.11	-4.66			
OZ-27	0.44	-4.26	Inf.	0.93	-4.70
OZ-28	0.13	-5.54			
OZ-29	0.94	-4.24			
OZ-30	1.17	-3.94	Vein	0.47	-5.84
OZ-31	0.47	-3.86			
OZ-32	0.67	-4.88			
OZ 33	1.34	-4.27			
OZ-34	1.57	-5.38			
OZ-35	2.78	-3.91			
OZ-36	2.83	-3.70			
OZ-37	2.49	-4.82			
OZ-38	2.07	-5.16			
OZ-39	2.76	-3.95			
Average	1.35	-4.35			
Mudurnu Section					
Samp. N.	$\delta^{13}C$	$\delta^{18}O$	Type	$\delta^{13}C$	$\delta^{18}O$
MY-24	3.44	-1.87			
MY-23	3.06	-2.37			
MY-22	3.24	-2.15			
MY-21	2.51	-3.81			
Average	3.06	-2.55			

Table 2: *Continued.*

Zonguldak-Çengellidere Section					
Samp. N.	**$\delta^{13}C$**	**$\delta^{18}O$**	**Type**	**$\delta^{13}C$**	**$\delta^{18}O$**
OCG-40	1.90	-3.46			
OCG-39	-0.20	-3.15	Inf.	1.43	-3.64
			Coral	0.55	-4.15
OCG-38	0.56	-5.31			
OCG-37	0.64	-5.57			
OCG-36	0.60	-3.41	Vein	0.39	-8.32
			Inf.	1.38	-3.08
			Coral	0.26	-3.76
OCG-32	1.03	-5.04			
OCG-31	1.91	-4.31			
OCG-30	0.29	-5.76			
OCG-29	-1.56	-6.30			
OCG-28	-1.05	-8.13			
OCG-27	1.31	-5.43			
OCG-26	0.51	-9.77			
OCG-25	1.88	-5.82	Vein	0.99	-7.20
OCG-24	1.57	-4.18			
OCG-23	2.67	-5.75			
OCG-22	2.67	-5.31	Shell	4.38	-2.76
OCG-21	2.15	-5.41			
OCG-14	2.87	-5.00			
OCG-13	1.99	-7.06			
OCG-12	2.02	-5.44	Vein	1.23	-8.17
			Shell	1.55	-5.18
OCG-11	0.95	-8.23			
OCG-10C	2.67	-5.30			
OCG-10B	2.79	-6.17	Shell	1.03	-4.26
OCG-10A	3.05	-5.93			
Averages	1.38	-5.63			

Zonguldak-Kozlu Section					
Samp. N.	**$\delta^{13}C$**	**$\delta^{18}O$**	**Type**	**$\delta^{13}C$**	**$\delta^{18}O$**
OZV 1A	0.59	-5.89	Vein	0.71	-8.72
OZV-1	0.01	-5.55			
OZV 2	-0.37	-5.04			
OZV 3	0.12	-4.53			
OZV 4	-0.06	-5.22			
OZV 5	0.04	-5.77			
OZV 6	-1.24	-7.08			
OZV 7	-0.52	-5.33	Vein	-0.89	-6.05
OZV 8	0.72	-5.49	Inf.	-0.23	-8.32
OZV 9	-0.38	-5.16			
OZV 10	-0.51	-3.27			
OZV-11A	0.71	-5.51			
OZV-11B	1.20	-5.42			
OZV-11C	0.83	-4.88			
OZV-12A	1.34	-4.46			
OZV-12B	1.15	-5.45			
OZV-12C	-0.35	-5.79			
OZV-13	1.19	-5.47			
OZV-14	0.07	-5.82			
OZV-15	0.36	-5.01			
OZV-16	-0.07	-5.08			
OZV-17	0.03	-5.09			
OZV-18	0.14	-6.93	Vein	-0.60	-10.68
Averages	0.20	-5.33			

Averages	$\delta^{13}C$	$\delta^{18}O$
Veins	-1.90	-6.78
Pelagics	2.19	-3.55
Platform Carbonates	0.84	-5.03
Host rock for Infillings	0.39	-4.08
Infillings	0.88	-4.94
Host rock for clasts	-1.15	-3.64
Clasts	-1.16	-3.87
Host rock for bioturbations	2.08	-3.52
Bioturbation	2.04	-3.72
Host rock for corals and shells	1.58	-4.70
Corals and shells	1.55	-4.02

Stable isotope data

The carbon isotope values for bulk rock samples in pelagic successions range from 0 ‰ to +4.2 ‰, oxygen isotope values in pelagic successions range from –5.3 ‰ to –1.9 ‰, with most samples having values between –2 and –4 ‰. For samples from platform successions, carbon isotope values for bulk rock samples vary between –2.26 ‰ and +3.05 ‰. Oxygen isotope values for inner platform successions range from –9.7 ‰ to –2.6 ‰, with most samples having values between –3 and –6 ‰. The carbon isotope values for vein samples range from +1.2 ‰ to –5.2 ‰, and oxygen isotope values range between –10.7 ‰ and –4.2 ‰ (Table 2).

Effects of diagenesis

The stable isotope compositions of carbonates can be significantly modified through diagenesis. Whether or not alteration of the isotopic composition occurs during recrystallization is a function of the original mineralogical constitution of the carbonate (e.g. metastable aragonite and high-Mg calcite versus low-Mg calcite; Patterson & Walter 1994), the isotopic composition of the fluid, and the temperature during alteration and recrystallization. Recrystallization, in the presence of meteoric water, tends to lower both the $\delta^{13}C$ and $\delta^{18}O$ values of carbonates (e.g. Lohmann 1988). The diagenetic history of the sections shows two different general patterns between the platform and pelagic sections in this study. The platform carbonates mainly composed of lime mudstone, wackestone, packstone display development of marine diagenesis (including cement A and B of Flügel 1982 in some parts) at the bottom and mid-parts of the cycle and meteoric diagenesis at the top of the cycle where subaerial exposure structures are developed. However, pelagic carbonates do not present any meteoric diagenesis along the sections and are mainly dominated by primary micrites. Joachimski (1994) states that micrites have a good potential for preservation of their primary carbon isotopic composition if the duration of subaerial exposure is rather brief.

By comparison to other carbonates analysed from Cretaceous sequences and considered to represent primary isotopic compositions (e.g. Weissert & Lini 1991; Menegatti & Weissert 1998; Stoll & Schrag 2000; Pittet et al. 2002) the $\delta^{18}O$ values of the sampled profiles are generally lower and hence are interpreted as having been affected by diagenesis. Support for a diagenetic influence on the bulk rock isotopic compositions is also given by a comparison of the isotopic compositions of the bulk rock with those measured from individual shells, corals, bivalves, and small veins within the same sections (Fig. 15 and Table 2). Shells, corals, and bivalves are on average, somewhat enriched in ^{18}O compared to their parent bulk rocks (Fig. 15 and Table 2). In contrast, late genetic veins in platform and pelagic carbonate samples are always significantly depleted in ^{18}O and C^{13} compared to the bulk rock (Fig. 15), indicating the influence of meteoric water in veins. The average carbon isotope compositions of clasts, shells, and corals are similar to average values of their host rocks. Furthermore, the carbon isotope compositions have a range that is very similar to that of other Cretaceous carbon-

ates and as illustrated in Figure 14a and discussed further below, the variations in $\delta^{13}C$ values of the Nallıhan section also correlate with global Aptian $\delta^{13}C$ curves (Weissert & Lini 1991; Weissert & Bréhéret 1991; Menegatti & Weissert 1998, and many others). These features, in addition to the observation that there is little co-variation in $\delta^{13}C$- and $\delta^{18}O$-isotope compositions (Fig. 15), and that the pelagic carbonates still retain higher average $\delta^{18}O$ values (–3.55 ‰) compared to the inner platform shallow water carbonates (–5.03 ‰) (Fig. 15 and Table 2), but with a parallel stratigraphic variation, indicate that the diagenetic influence was limited. Thus, while a diagenetic influence may somewhat shift oxygen isotope values, the original variations are still preserved.

Other possible effects causing variations of $\delta^{13}C$ and $\delta^{18}O$ values can be changes in ocean water circulation, changes in amount of terrestrial input, rate of carbonate productivity, and/or salinity changes (De Boer 1982).

Similar cyclic isotope curves are obtained from peritidal carbonates of the isolated platform (Taurides), from shallow marine deposits of the continental shelf (Zonguldak) and from pelagic successions (Sakarya). This is explained by common mechanisms for all studied settings. Eustatic sea level changes in relation to climatic variations appear to be the most likely factors. The marl/limestone couplets showing similar cyclic isotope curves with their shallow water counterparts (Fig. 14b) indicate the presence of small-scale sea level changes induced by short-term climatic fluctuations and the positions of limestone-marl/shale facies within a cycle become clearer.

The relationship between stable isotope compositions and sea level changes

Stable isotope compositions were measured with the aim of determining the mechanisms responsible for the meter-scale shallowing-upward cycles in platform carbonates and the limestone-marl couplets in pelagic successions. Many studies have concentrated on the causes of cyclicity within Cretaceous sediments deposited under what is often considered a relatively equable greenhouse-type climate (e.g. Einsele et al. 1991; De Boer & Smith 1994; Miall 1997; Einsele 2000; Fiet et al. 2001; Strasser et al. 2001). Some of the studies suggest-

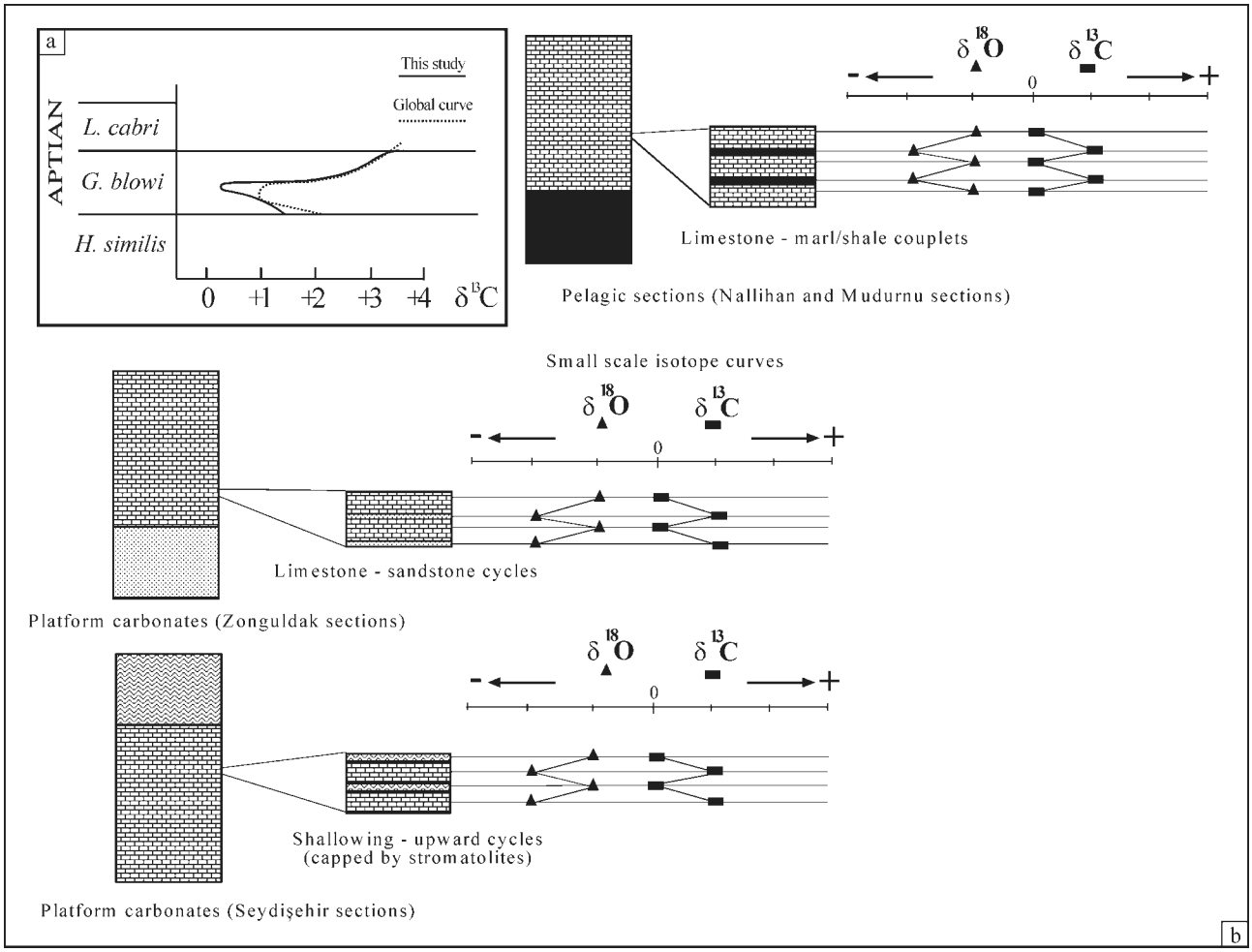

Fig. 14. **a** — Comparison of the $\delta^{13}C$ curves in *G. blowi* Zone. The dotted line represents the global curve (Wiessert & Lini 1991; Menegatti & Weissert 1998 and many others), the solid line represents the carbon isotope curve in this study. Curves are smoothed and simplified. **b** — Representative diagram illustrating small-scale and large-scale facies and stable isotope synchronicity in pelagic and inner platform settings in this study.

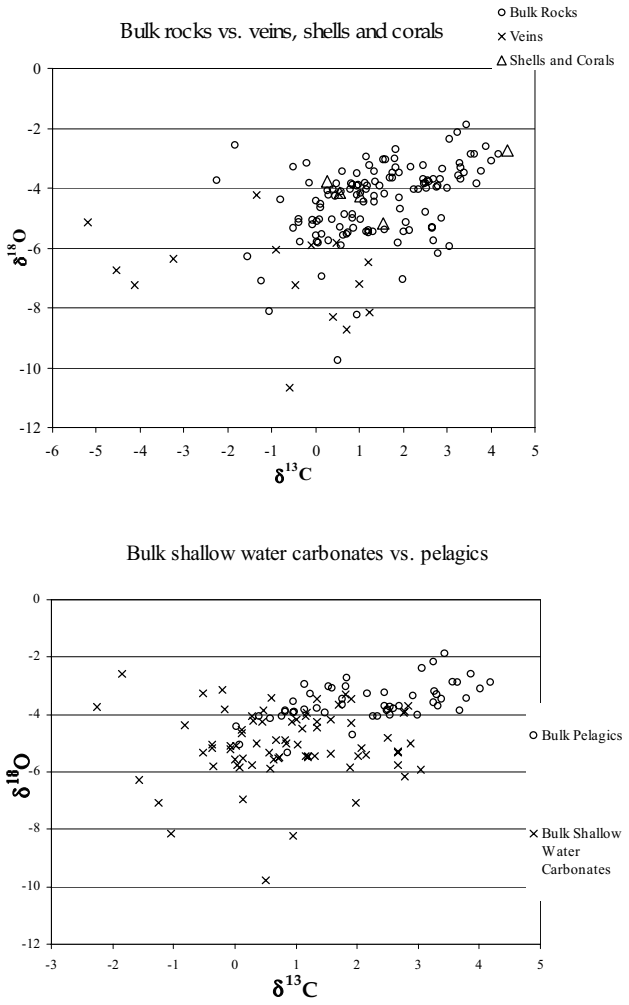

Fig. 15. Graphic expressions of relationships between carbon and oxygen stable isotope compositions of bulk rock samples, veins, shells and corals (data from Table 2).

ed fluctuating glacial activities within a greenhouse Cretaceous (Weissert & Bréhéret 1991; Weissert & Lini 1991; Selwood et al. 1994; Pirrie et al. 1995; Jenkyns & Wilson 1999; Price 1999; Stoll & Schrag 2000). Therefore, waxing or waning ice volumes even during Cretaceous greenhouse conditions may be the most apparent cause for fluctuating eustatic sea levels. Strasser et al. (1999) stated that thermal expansion and retraction of the uppermost layer of ocean water by thermally induced volume changes in deep water circulation might have contributed to high-frequency sea level variations, and also noticed that a "cool mode" in paleoclimate from Middle Jurassic to Early Cretaceous with a pronounced seasonality was present, and although ice-volumes were not sufficient to introduce important glacio-eustatic fluctuations, they could make small contributions.

Changes towards more positive $\delta^{18}O$ values can be interpreted as a result of lowering of eustatic sea level caused by cooling episodes and build up of ice-sheets, while changes towards more negative $\delta^{18}O$ values may be correlated with a rise in sea level, corresponding to warming episodes. In addition to changes in $\delta^{18}O$ values, changes in the $\delta^{13}C$ values of carbonates may also be linked to changes in climate as the carbon isotope compositions are ultimately linked to the carbon cycle and the bioproductivity in the water column of the Cretaceous ocean (e.g. Weissert & Lini 1991). Hence, changes towards lower $\delta^{13}C$ values may be associated with lower biological productivity, which in turn may be related to reduced nutrient flux and water cycle and overall cooling.

For the sedimentary cycles of the Taurides (Seydişehir), the Pontides (Zonguldak), as well as the pelagic Mudurnu Trough carbonates, the variations in $\delta^{18}O$ values are all similar in that they generally increase in parallel with the shallowing-upward cycles (Figs. 7 to 13, 14a,b). The overlying cycle returns to lower, more negative $\delta^{18}O$ values at the bottom and again ends up with higher values towards the top. This is the case even though the cycles are composed of different lithofacies in different settings. This pattern is recorded in most of the cycles and, despite the diagenetic overprint, can be interpreted as a record of changing sea level and temperature as a result of changes in the ice-volume. Hence, transgressive portions of the cycles with lower $\delta^{18}O$ values indicate warmer periods, whereas regressive portions of cycles with more positive $\delta^{18}O$ values indicate cooler periods. This relationship is also observed on the scales of the smallest cycles recognized, with changes in $\delta^{18}O$ being on the order of about 1 ‰ for smaller cycles to about 2 ‰ for larger cycles.

While changes in the $\delta^{13}C$ values are not as constant with regard to the direction of change within a cycle compared to those for $\delta^{18}O$ values, there is nonetheless also a general tendency to have more positive values in the transgressive portions and more negative values in the regressive portions of the cycles. This also supports the idea of warming during the transgressive phase and cooling during the regressive phase. However, there are also a number of cycles where the changes in $\delta^{13}C$ values with respect to the transgressive-regressive cycles are not as clear. This is likely to be related to other factors besides climate affecting the bioproductivity in the water column as well as complex changes in the types of organisms and their relative abundances as a function of time and sedimentary facies, and pedogenetic alterations at the top of the subaerially exposed cycles.

The curve depicting the $\delta^{13}C$ values of the pelagic Nallıhan section, the most complete section sampled in this study (Fig. 13), is quite comparable to other Aptian $\delta^{13}C$ curves, both in terms of the magnitude of change in $\delta^{13}C$ values (0 ‰ to +4 ‰) and in terms of the absolute $\delta^{13}C$ values (Fig. 14a) (Weissert & Bréhéret 1991; Weissert & Lini 1991; Ferreri et al. 1997; Grötsch et al. 1998; Kuhnt et al. 1998; Jenkyns & Wilson 1999; Erba et al. 1999; Strasser et al. 2001). The Nallıhan section includes a prominent black shale interval within the *G. blowi* Zone. This position of this black shale is directly comparable to the "Selli level", which marks a prominent large-scale transgressive event in sections studied elsewhere (Menegatti & Weissert 1998). The correlation to other sections where this event has been interpreted as being related to a large-scale transgression also supports the conclusion that the marl-shale sequences within the cycles are related to small-scale rises in sea level (Yılmaz et al. 2000; and Yılmaz 2002).

The variations in $\delta^{18}O$ values observed for the small cycles as well as the larger cycles (Figs. 7 to 13, 14) imply that small-scale variations of climate and sea level were superim-

posed over larger-scale variations. Hence, even during the Cretaceous greenhouse-type climate, significant short-term variations were possible, and the climate during the Cretaceous was not as equable as previously thought.

The Tauride and Pontide platforms are interpreted to have formed in tropical-subtropical belts during the Early Cretaceous. The shallow water carbonates of these platforms display a warm-water facies. No cool-water carbonate facies has been recorded in the studied sections. However, cooling periods are interpreted from the stable isotope variations measured in these sections. This implies that temperature changes were not sufficiently large to change the character of the facies in the tropical-subtropical regions, but large enough to cause sufficient melting in the polar regions in order to affect sea level and the oxygen isotope composition of the seawater.

Conclusions

In this study, changes in the C and O isotope composition of Barremian-Aptian platform carbonates of the Taurides and Pontides and their pelagic counterparts are documented. $\delta^{18}O$ values generally change towards more positive values at the top of the cycle, but again more negative at the base of the next cycle. This cyclicity in $\delta^{18}O$ values is interpreted as a primary variation reflecting changes in temperature and sea level on the order of the Milankovitch frequency band. Meter-scale cycles of inner platform carbonates and of pelagic successions are thus likely to be related to small-scale changes in glacial activity and/or thermal expansion of the ocean water. $\delta^{13}C$ values are more difficult to interpret for the small-scale cycles, but on a larger scale the $\delta^{13}C$ curve compares well with the ones measured for the same time interval. This is particularly the case for the pelagic Nallıhan section, which can be correlated on a global scale and for which the changes in values are of similar magnitude.

The C and O isotope compositions measured in the sections of this study can thus be interpreted to reflect primary variations, even though the primary compositions have been slightly modified by diagenetic changes. Such changes appear to have had a more pronounced effect on the oxygen rather than the carbon isotope compositions.

Acknowledgments: This work was supported by the Turkish Scientific and Technical Research Council (TÜBITAK, (Project No: YDABÇAG-198Y040) Ankara, Turkey) and the Middle East Technical University (Ankara, Turkey), and by the Institute of Mineralogy, Petrology, and Geochemistry of the University of Tübingen (Germany). We thank Prof. Dr. André Strasser (Fribourg, Switzerland), Dr. Otília Lintnerová (Bratislava, Slovak Republic) and Prof. Dr. Okan Tüysüz (Avrasya Yerbilimleri Enstitüsü, İTÜ, Turkey) for the review of the manuscript. We are grateful to Necdet Özgül (Geomar, Istanbul) for sharing his experiences during fieldwork and to Yakup Özcelik (TPAO, Ankara) for his help in characterizing the well-exposed sections in the Zonguldak region. We also want to thank Bernd Steinhilber (University of Tübingen) for his help with the laboratory work.

References

Altıner D. 1991: Microfossil biostratigraphy (mainly foraminifers) of the Jurassic–Lower Cretaceous carbonate successions in Northwestern Anatolia (Turkey). *Geol. Romana* 27, 167–215.

Altıner D. & Decrouez D. 1982: Etude stratigraphique et micropaléontologique du Crétacé de la région au NW de Pınarbaşı (Taurus Oriental, Turquie). *Rev. Paleobiol.* 1, 53–91.

Altıner D. & Özkan S. 1991: Calpionellid zonation in North-Western Anatolia (Turkey) and calibration of the stratigraphic ranges of some benthic foraminifera at the Jurassic–Cretaceous boundary. *Geol. Romana* 27, 215–235.

Altıner D., Koçyiğit A., Farinacci A., Nicosia U. & Conti M.A. 1991: Jurassic–Lower Cretaceous stratigraphy and paleogeographic evolution of the southern part of North-Western Anatolia (Turkey). *Geol. Romana* 27, 13–81.

Altıner D., Yılmaz İ.Ö., Özgül N., Akcar N., Bayazıtoğlu M. & Gaziulusoy Z. 1999: High resolution sequence stratigraphic correlation in the Upper Jurassic (Kimmeridgian)–Upper Cretaceous (Cenomanian) peritidal carbonates deposits (Western Taurides, Turkey). In: Bozkurt E. & Rowbotham G. (Eds.): Advances in Turkish geology. Part I: Tethyan evolution and fluvial-marine sedimentation. *Geol. J. Spec. Issue* 34, 139–158.

Altıner D. & Yılmaz İ.Ö. 2000: Foraminiferal diversification within the sequential development of Upper Jurassic–Lower Cretaceous peritidal carbonates (Western Taurides, Turkey). *6th International Cretaceous Symposium, Abstract Book* 9, Vienna.

Barrera E. & Johnson C.C. 1999: Evolution of the Cretaceous ocean-climate system. *Geol. Soc. Amer., Spec. Pap.* 332, 1–445.

Bellonca A., Claps M., Erba E., Masetti D., Neri R., Silva I.P. & Venezia F. 1996: Orbitally induced limestone/marlstone rhythms in the Albian-Cenomanian Cismon section (Venetian region, northern Italy): Sedimentology, calcareous and silicious plankton distribution, elemental and isotope geochemistry. *Palaeogeogr. Palaeoclimatol. Palaeoecol.* 126, 227–260.

Bralower T.J., Arthur M.A., Leckie R.M., Sliter W.V., Allard D.J. & Schlanger S.O. 1994: Timing and paleoceanography of oceanic dysoxia/anoxa in the Late Barremian to Early Aptian (Early Cretaceous). *Palaios* 9, 335–369.

Bralower T.J., CoBabe E., Clement B., Sliter W.V., Osburn C.L. & Longoria J. 1999: The record of global change in Mid-Cretaceous (Barremian-Albian) sections from the Sierra Madre, Northern Mexico. *J. Foram. Res.* 29, 418–437.

Claps M. & Masetti D. 1994: Milankovitch periodicities recorded in Cretaceous deep sea sequences from the southern Alps (Northern Italy). In: De Boer P.L. & Smith D.G. (Eds.): Orbital forcing and cyclic sequences. *Spec. Publ. Inter. Assoc. Sedimentologists* 19, 99–109.

Claps M., Erba E., Masetti D. & Melchiorri F. 1995: Milankovitch-type cycles recorded in Toarcian black shales from the Belluno trough (southern Alps, Italy). *Mem. Sci. Geol.* 47, 179–188.

De Boer P.L. 1982: Some remarks about the stable isotope composition of cyclic pelagic sediments from the Cretaceous in the Apennines (Italy). In: Schlanger S.O. & Cita M.B. (Eds.): Nature and origin of Cretaceous carbon-rich facies. *Academic Press,* London, 129–144.

De Boer P.L. & Smith D.G. 1994: Orbital forcing and cyclic sequences. *Spec. Publ. Internal Assoc. Sedimentologists* 19, 1–559.

Demicco R.V. & Hardie L.A. 1994: Sedimentary structures and early diagenetic features of shallow marine carbonate deposits. *S.E.P.M. Atlas Series* 1, 1–265.

Derman A.S. 1990: Late Jurasic and Early Cretaceous geological evolution of the Western Black Sea region, Turkey. *8th Petroleum Congress and Exhibition of Turkey, Proceedings*, Ankara 328–340.

Einsele G. 2000: Sedimentary basins: evolution, facies and sediment budget. *Springer-Verlag*, Berlin, 1–792.

Einsele G., Ricken W. & Seilacher A. 1991: Cycles and events in stratigraphy. *Springer-Verlag*, Berlin, 1–955.

Erba E., Channell J.E.T., Claps M., Jones C., Larson R., Opdyke B., Premoli-Silva I., Riva A., Salvini G. & Torricelli S. 1999: Integrated stratigraphy of the Cismon Apticore (southern Alps, Italy): a "reference section" for the Barremian-Aptian interval at low latitudes. *J. Foram. Res.* 29, 371–391.

Ferreri V., Weissert H., D'Argenio B. & Buonocunto F.P. 1997: Carbon isotope stratigraphy: a tool for basin to carbonate platform correlation. *Terra Nova* 9, 57–61.

Fischer A.G. 1991: Orbital cyclicity in Mesozoic strata. In: Einsele G., Ricken W. & Seilacher A. (Eds.): Cycles and events in stratigraphy. *Springer-Verlag,* Berlin, Heidelberg, 48–62.

Fiet N., Beaudoin B. & Parize O. 2001: Lithostratigraphic analysis of Milankovitch cyclicity in pelagic Albian deposits of central Italy: implications for the duration of the stage and substages. *Cretac. Research* 22, 265–275.

Flügel E. 1982: Microfacies analysis of limestones, *Springer-Verlag,* Berlin, Heidelberg, 1–633.

Görür N. 1997: Cretaceous syn-to-postrift sedimentation on the southern continental margin of the western Black Sea basin. In: Robinson A.G. (Ed.): Regional and petroleum geology of the Black Sea and sorruonding region. *A.A.P.G. Memoir* 68, 227–240.

Grötsch J., Billing I. & Vahrenkamp V. 1998: Carbon-isotope stratigraphy in shallow-water carbonates: implications for Cretaceous black-shale deposition. *Sedimentology* 45, 623–634.

Graciansky P.-C. de, Hardenbol J., Jacquin T. & Vail P.R. 1998: Mesozoic and Cenozoic sequence stratigraphy of European basins. *S.E.P.M. Spec. Publ.* 60, 1–786.

Haq B.U., Hardenbol J. & Vail P.R. 1988: Mesozoic and Cenozoic chronostatigraphy and cycles of sea-level change. In: Wilgus C.K. & Hastings B.S. et al. (Eds.): Sea level changes: An integrated approach. *S.E.P.M. Spec. Publ.* 42, 71–108.

Hesselbo S.P. & Huggett J.M. 2001: Glaucony in ocean-margin sequence stratigraphy (Oligocene-Pliocene, Offshore New Jersey, U.S.A., ODP Leg 174A). *J. Sed. Res.* 71, 4, 599–607.

Jenkyns H.C. & Wilson P.A. 1999: Stratigraphy, paleoceanography, and evolution of Cretaceous pacific guyots: relics from a greenhouse earth. *Amer. J. Sci.* 299, 341–392.

Joachimski M.M. 1994: Subaerial exposure and deposition of shallowing upward sequences: evidence from stable isotopes of Purbeckian peritidal carbonates (basal Cretaceous), Swiss and French Jura Mountains. *Sedimentology* 41, 805–824.

Kaya O., Dizer A., Tansel İ. & Meriç E. 1983: Cretaceous stratigraphy of Ereğli (Zonguldak) region. *Bull. Miner. Res. Explor. Inst. Turkey* 99, 100, 19–32.

Kuhnt W., Moullade M., Masse J-P. & Erlenkeuser H. 1998: Carbon isotope stratigraphy of the Lower Aptian historical stratotype at Cassis-La Bédoule (SE France). *Géologie Méditerranéenne* 25, 63–79.

Larson R.L. & Erba E. 1999: Onset of the mid-Cretaceous greenhouse in the Barremian–Aptian: igneous events and the biological, sedimentary, and geochemical responses. *Paleoceanography* 14, 663–678.

Lohmann K.C. 1988: Geochemical patterns of meteoric diagenesis system and their application to paleokarst. In: Choquette P.W. & James N.P. (Eds.): Paleokarst. *Springer-Verlag*, New York, 58–80.

Martire L. 1992: Sequence stratigraphy and condensed pelagic sediments. An example from the Rosso Ammonitico Veronese, northeastern Italy. *Palaeogeog. Palaeoclimatol. Palaeoecol.* 94, 169–191.

Menegatti A.P. & Weissert H. 1998: High-resolution δ^{13} C stratigraphy through the Early Aptian "Livello Selli" of the Alpine Tethys. *Paleoceanography* 13, 530–545.

Miall A.D. 1997: The geology of stratigraphic sequences. *Springer-Verlag*, Berlin, 1–433.

Monod O. 1977: Geological researches of eastern Taurus at south of Beyşehir (Turkey). *These,* Universite Paris XI Orsay, 1–422 (in French).

Mutterlose J. & Ruffell A. 1999: Milankovitch-scale palaeoclimate changes in pale–dark bedding rhythms from the early cretaceous (Hauterivian and Barremian) of eastern England and northern Germany. *Palaeogeog. Palaeoclimatol. Palaeoecol.* 154, 133–160.

Orhan E. 1995: General geology of Zonguldak coal basin and stratigraphy of Kozlu K20/G borehole. In: Yalcın N.M. & Gürdal G. (Eds.): Exploration boreholes in Zonguldak-1: Kozlu — K20/G. TÜBÝTAK, MAM, (Turkish Scientific and Technical Research Council, Marmara Research Center). *Earth Sci. Sect. Spec. Publ.* 45–66 (in Turkish).

Osleger D.A. 1991: Subtidal carbonate cycles: implications for allocyclic vs. autocyclic controls. *Geology* 19, 917–920.

Önal M., Helvacı C., İnci U., Yağmurlu F., Meriç E. & Tansel İ. 1988: Stratigraphy, age, lithofacies and depositional environments of Soğukçam Limestone, Nardin Formation and Kızılçay Group in Çayırhan at the north of north western part of Ankara. *Bull. Turkish Petroleum Geologists Assoc.* 1/2, 152–163 (in Turkish).

Özgül N. 1983: Stratigraphy and tectonic evolution of the central Taurids. In: Tekeli O. & Göncüoğlu C. (Eds.): Geology of the Taurus Belt. Printed by *Miner. Res. Explor. Inst.,* Ankara, 77–90.

Özgül N. 1997: Stratigraphy of tectono-stratigraphic units located in around Bozkır-Hadim-Taşkent (Northern part of central Taurides). *Bull. Miner. Res. Explor. Inst. Turkey* 119, 113–174 (in Turkish).

Patterson W.P. & Walter L.M. 1994: Depletion of ^{13}C in sea water CO_2 on modern carbonate platform: significance for the carbon isotopic record of carbonates. *Geology* 22, 885–888.

Peybernes B., Ivanov M., Nikolov T., Ciszak R. & Stoykova K. 2000: Depositional sequences at the Urgonian platform/basin transition (Barremian-Albian interval) in the western Fore-Balkan (northwest Bulgaria). *Comptes Rendus de l Academie des Sciences Serie II Fascicule A-Sciences de la Terre et des Planetes* 330, 8, 547–553.

Pirrie D., Doyle P., Marshall J.D. & Ellis G. 1995: Cool Cretaceous climate: new data from the Albian of western Australia. *J. Geol. Soc.*152, 739–742.

Pittet B., Van Buchem F.S.P., Hillgärtner H., Razin P., Grötsch J. & Droste H. 2002: Ecological succession, paleoenvironmental change, and depositional sequences of Barremian–Aptian shallow water carbonates in northern Oman. *Sedimentology* 49, 555–581.

Price G.D. 1999: The evidence and implications of polar ice during the Mesozoic. *Earth Sci. Rev.* 48, 183–210.

Premoli Silva I. & Sliter W.V. 1999: Cretaceous paleoceanography; evidence from planktonic foraminiferal evolution. In: Barrera E. & Johnson C.C. (Eds): Evolution of the Cretaceous ocean-climate system. *Geol. Soc. Amer., Spec. Pap.* 332, 301–328.

Prokoph A. & Thurow J. 2001: Orbital forcing in a "Boreal" Cretaceous epieric sea: high-resolution analysis of core and logging data (Upper Albian of Kirchrode-I drill core — Lower Saxony Basin, NW Germany). *Palaeogeogr. Palaeoclimatol. Palaeoecol.* 174, 67–96.

Raspini A. 2001: Stacking pattern of cyclic carbonate platform strata: Lower Cretaceous of southern Appennines, Italy. *J. Geol. Soc.* 158, 353–366.

Selwood B.W., Price G.D. & Valdes P. J. 1994: Cooler estimates of Cretaceous temperatures. *Nature* 370, 453–455.

Stoll H.M. & Schrag D.P. 2000: High-resolution stable isotope records from the Upper Cretaceous rocks of Italy and Spain: Glacial episodes in a greenhouse planet? *Geol. Soc. Amer. Bull.* 112, 308–319.

Strasser A. 1991: Lagoonal-peritidal sequences in carbonate environments: autocyclic and allocyclic processes. In: Einsele G., Ricken W. & Seilacher A. (Eds.): Cycles and events in stratigraphy. *Springer-Verlag*, Berlin, Heidelberg, 709–721.

Strasser A., Caron M. & Gjermeni M. 2001: The Aptian, Albian and Cenomanian of Roter Sattel, Romandes Prealps, Switzerland: a high-resolution record of oceanographic changes. *Cretac. Research* 22, 173–199.

Strasser A., Pittet B., Hillgärtner H. & Pasquier Jean-Bruno 1999: Depositional sequences in shallow water carbonate — dominated sedimentary systems: concepts for a high-resolution analysis. *Sed. Geol.* 128, 201–221.

Şengör A.M.C. & Yılmaz Y. 1981: Tethyan evolution of Turkey: A plate tectonic approach. *Tectonophysics* 75, 181–241.

Tokay M. 1954/55: Géologie de la région de Bartın (Zonguldak-Turquie du Nord). *Bull. Miner. Res. Explor. Inst. Turkey* 46, 47, 46–64.

Vennin E. & Aurell M. 2001: Aptian paleoenvironmental evolution and sequence stratigraphy in the Galve sub-basin (Teruel, NE Spain). *Bull. Soc. Géol. France* 172, 4, 397–410.

Weissert H. & Lini A. 1991: Ice age interludes during the time of Cretaceous greenhouse climate?. In: Müller D.W., McKenzie J.A. & Weissert H. (Eds.): Controversies in modern geology. *Academic Press Limited*, New York, 173–191.

Weissert H. & Bréhéret J.G. 1991: A carbonate carbon-isotope record from Aptian-Albian sediments of the Vocontian trough (SE France). *Bull. Soc. Géol. France* 162, 1133–1140.

Wezel F.C. 1985: Anoxic facies of global geotectonic episodes. *G. Geol., Ser., 3a*. 47, 281–286 (in Italian).

Yılmaz İ.Ö. 1999: Taxonomic and paleogeographic approaches to the dasyclad algae in the Upper Jurassic (Kimmeridgian)–Upper Cretaceous (Cenomanian) peritidal carbonates of the Fele (Yassıbel) area (Western Taurides, Turkey). *Turkish J. Earth Sci.* 8, 81–101.

Yılmaz İ.Ö. 2002: Applications of cyclostratigraphy and sequence stratigraphy in determination of the hierarchy in peritidal and pelagic successions (NW, SW and WNW of Turkey) by using sedimentology and sedimentary geochemistry (stable isotopes). *Ph.D. Thesis, Department of Geological Engineering, Middle East Technical University*, Ankara, 1–248.

Yılmaz İ.Ö. & Altıner D. 2000: Cyclicity and eustatic controls on the carbonate peritidal deposits (Upper Jurassic (Kimmeridgian)–Upper Cretaceous (Cenomanian)) of the Fele area (Western Taurides, Turkey). *Sediment 2000, 15th Meeting of Sedimentologists, Abstract Book.* Leoben, Austria, 152.

Yılmaz İ.Ö. & Altıner D. 2001: Use of sedimentary structures in the recognition of sequence boundaries in the Upper Jurassic (Kimmeridgian)–Upper Cretaceous (Cenomanian) peritidal carbonates of the Fele (Yassıbel) area (Western Taurides, Turkey). *Int. Geol. Rev.* 43, 8, 736–753.

Yılmaz Y., Tüysüz O., Yigitbas E., Genc S.C. & Sengör A.M.C. 1997: Geology and tectonic evolution of the Pontides. *A.A.P.G. Memoir* 68, 183-226.

Yılmaz İ.Ö., Altıner D. & Özkan-Altıner S. 2000: Record of Milankovitch cyclicity within the Barremian-Aptian pelagic successions of NW Turkey: Preliminary results. *6th International Cretaceous Symposium, Abstract Book.* Vienna, Austria, 153.